TECHNICAL AND VOCATIONAL TRAINING INSTITUTE (TVTI)

School of Graduate Studies

FACULTY OF ELECTRICAL AND ELECTRONICS TECHNOLOGY AND INFORMATION AND COMMUNICATION TECHNOLOGY (DEPARTMENT OF ELECTRICAL AND ELECTRONICS TECHNOLOGY)

Simulation of Motion Control Differential Drive Mobile Robots Using Global Terminal Sliding Mode Controller.

MSc Thesis for the Partial Fulfillment of

Master of Science in Electrical Automation and Control Technology Management

By,

Bahiru Befekadu (MTR/477/13)

Supervisor,

Beteley Teka (PhD)

AUGUST 2022

Addis Ababa, Ethiopia

Simulation of Motion Control Differential Drive Mobile Robots Using Global Terminal Sliding Mode Controller.

A Thesis submitted to

TECHNICAL AND VOCATIONAL TRAINING INSTITUTE (TVTI)

FACULTY OF ELECTRICAL AND ELECTRONICS TECHNOLOGY AND INFORMATION AND COMMUNICATION TECHNOLOGY (DEPARTMENT OF ELECTRICAL AND ELECTRONICS TECHNOLOGY)

In partial fulfillment for the Degree

MASTER OF SCIENCE *in* ELECTRICAL AUTOMATION AND CONTROL TECHNOLOGY MANAGEMENT

By,

Bahiru Befekadu (MTR/477/13)

Supervisor,

Beteley Teka (PhD)

DECLARATION

I, the undersigned, declare that this thesis work is my original work, has not been presented for a degree in this or any other universities, and all sources of materials used for the thesis work have been fully acknowledged.

_____ _____

Bahiru Befekadu Signature

Place: Addis Ababa TVTI

This thesis has been submitted for examination with my approval as a university advisor.

_____ _____

Advisor's Name Signature

TECHNICAL AND VOCATIONAL TRAINING INSTITUTE (TVTI)
FACULTY OF ELECTRICAL AND ELECTRONICS TECHNOLOGY AND INFORMATION AND COMMUNICATION TECHNOLOGY
(DEPARTMENT OF ELECTRICAL AND ELECTRONICS TECHNOLOGY)

Thesis on

Simulation of Motion Control Differential Drive Mobile Robots Using Global Terminal Sliding Mode Controller.

By,
Bahiru Befekadu (MTR/477/13)

APPROVED BY THESIS ADVISOR COMMITTEE

Name of the Advisor	Signature	Date
---	---	---
Name of Examiner Internal	Signature	Date
---	---	---
Name of Examiner, Internal	Signature	Date
---	---	---
Name of Examiner, External	Signature	Date
---	---	---
Name of Chairperson	Signature	Date
---	---	---

ACKNOWLEDGEMENT

I am grateful acknowledgment and thank all of those who associated me my thesis writing at Technical Vocational Training Institute (TVTI). First I would like to thank Dr. Beteley Teka my advisor from Head of the department (HoD), defense University College of Engineering .Have been appreciated his guidance ,patient and personal time through my thesis writing .Special thanks are given to other graduate study committee coordinator and participants.

ABSTRACT

The primary goal of this study was to model and design a global fast terminal sliding mode control with quick reaching strategy for a two-wheeled mobile robots, specifically for differential drive mobile robot. In this thesis, an approach of dynamics modeling of DDMR using Langrage and GFTSMCQR trajectory tracking of DDMR is proposed. The proposed controller is a cascaded system such that designed to improve the dynamic response of the system i.e. fast convergence and high precision control system, asymptotical convergence, and chattering phenomena using GFTSMCQR. To render an asymptotical merging of the response to desired states and decrease the chattering in a traditional SMC system, a quick reaching law is proposed for DDMR, which makes the DDMR system have a fast approaching rate without chattering due switching functions. Moreover, an improved GFT sliding surface is proposed for the DDMR, makes DDMR translational and rotational system to attain equilibrium points in a finite time along the GFT sliding surface with an increased approaching rate and high precision control system. Therefore, for DDMR a GFTSMCQR is intended by implementing the proposed reaching control law and GFT sliding surface, which can accelerate the convergence rate of the system states in both of the phase, i.e. reaching and sliding phase. In this thesis, trajectory tracking motion control problems approach consists of kinematic level controller (outer level) and dynamic control (inner controller) which incorporates both kinematic and dynamic model of differential drive mobile robots respectively. Kinematic controller is designed based on two laws of control for DDMR, the first control law is for angular velocity and secondly, linear velocity which aims to bring the angular error and posture error to zero in a finite time using global fast terminal mode control approaches. Dynamic controller is designed to guarantee that error between the actual and desired rotation position to be zero, such that corresponding error between actual and desired velocity is approach to zero in a predetermined time using global fast terminal sliding surface with quick reaching law including matching model uncertainty. Finally, the algorithm's performance is demonstrated by model simulation and the proposed control, with simulation results indicating good convergence for circular trajectories from two different starting points.

Keywords: Differential drive mobile robot (DDMR); langrage approach, sliding mode control (SMC); trajectory tracking; global fast terminal slide mode control with quick reaching law (GFTSMCQR)

TABLE OF CONTENTS

LIST OF FIGURES

LIST OF TABLES

LIST OF ABBREVIATIONS

WMR	Wheel Mobile Robot
DDMR	Differential Mobile Robot
GFTSMCQR	Global Fast Terminal Sliding Mode Control Quick Reaching
FTRC	Fuzzy Target Reaching Control
PID	Proportional Integral Control
VSC	Variable Structure Control
LQ	Linear Quadratic
TMS	Terminal Sliding Mode
NGFSMC	Novel Global Fast Sliding Mode
NGFTSMC	Novel Global Fast Terminal Sliding Mode Control

LIST OF SPECIAL SYMBOLS

$v2$	Wheels voltage left wheel of the mobile plat form
θ	Rotational position of the mobile platform
$v1$	The voltage at right wheel of mobile platform
$\tau 2$	Torque at the second joint of manipulator
$\tau 1$	Torque at the first joint on the left
$fd2$	Upper disturbance on the left motor
$fd1$	Upper disturbance on right left motor
Y	Translational position along y-axis
x	Translational position along x-axis
φ	Wheel rotor
R	Radius of the driver wheel
D	The distance of the robot axle center and driving wheel
A	The distance between locations on the axle center
m_c	The wheel of the mobile robot
m_w	The combined mass of each xr axis driving wheel
I_C	The junction of the robot xr axis driving wheel motor and rotor
I_w	Rotational inertia of the motor rotor and each driving wheel
ρ	Right wheel rotor and left wheel position
T_{wr}	The right wheel kinetic energy
T_{wr}	The left wheel kinetic energy
Q	Generalized coordinate
fi	Generalized force
a_{ij}	Kinetic constraint

λ	Langragian multipliers
v	Linear velocity
ω	Angular velocity
e_2	Error for rotation position left wheel and mobile robot dynamic
θ_e	Equilibrium point
$\ddot{\theta}_\iota$	Control in put
$\dot{\phi}$	Driving radius rotation speed
ϕ	Encoder rotation
ε	Fixed robot
$\dot{y_r}$	Lateral slip
${v_i}^2$	generalized velocity inertia frame

CHAPTER ONE
INTRODUCTION

1.1. Background

The mobile control problem, which involves the kinematics, dynamics, and control of wheeled mobile robots, is becoming increasingly popular. From the beginning point to the goal position, the planner must deduce a free path. Once the path has been planned, the controller's task is to make sure that the robot follows it. Nonetheless, there are a variety of ways for developing mobile robot controllers. Because of their problems in control design and execution, control of wheeled mobile robots has piqued the interest of numerous robotics experts [1,2]. Many control methods have been presented to solve the challenge of tracking control of a mobile robot under Non-holonomic constraints in the previous decade [3, 4].

The Brockett theorem demonstrates that the latter cannot be stabilized by a continuous state feedback steady [1, 2], even though they are controllable in open loops, which restricts the use of the traditional theory of WMR. The emphasis of researchers has shifted from conventional control to design unconventional control [1]. The tracking control problem can be categorized along two axes and as a kinematic or dynamic problem depending on whether WMR is formulated using a kinematic or dynamic model [5]. However, the non-integrality of the Non-holonomic constraints makes it difficult to maintain the tracking control of mobile robot WMR [6]. As a result, in recent years, directing mobile robots has become a hot research area. The field of mobile robotics has become quite demanding due to the many applications of mobile robotics in our daily lives, particularly when safety, efficiency, and a big workforce are required.

Military, hostile environments (volcanic, biochemical, nuclear sites), and as helpful technology in rural regions, households, businesses, and industries are the principal applications for mobile robots. A modeling and control system for a mobile robot system, a two-wheeled mobile robot, or a mobile robot with differential drive (DDMR) is presented in this thesis. The differential drive-wheeled mobile robot’s consist of two wheels’ standard unicycle wheels actuated with motors and one caster wheels at the front and dynamics of proposed mobile robots derived by langrage formulation approach. A motion control system is designed for the DDMR using global fast terminal sliding mode control system. The first control law for angular velocity and linear velocity are proposed using global fast terminal sliding mode control to bring the robot's posture and angular error to zero in a finite time. Secondly, dynamic controller designed using proposed control system using GFTSMCQR.

1.2. Statement of problems

The field of mobile robotics is highly enabling, and researches in this area have extremely advanced across the world. Since, mobile robotics different tasks namely, arc welding, painting, environmental inspection, anti-weed spraying, nuclear plant, seed planting, and measurement of nitrogen content in soil and provide the necessary amount of fertilizer or any other relevant activity. For many communications, sensing, and control applications, precise and reliable modeling and control appear to be a necessary and crucial needed. Moreover, fast convergence and high precise control system required under both internal and external disturbances for different applications addressed above. A mobile robot is a highly nonlinear system, multivariable with highly coupled system this area high attractive research area in past decades.

However, some key issues exist that restrict the applications:

- The system may also be subjected to uncertain nonlinearities such as external disturbances, matching model uncertainty
- Convergence rate and precision of control system
- Asymptotical convergence and chattering phenomena in conventional sliding mode control system. Because, Traditional sliding mode control system is prone to problems such as asymptotical convergence and chattering both in sliding surfaces and reaching phase.
- considered only its kinematic model for position control of mobile robot using kinematic control system ignoring the effects of dynamics of mobile robots because, in practice perfect velocity control system is impossible without considering dynamics of mobile robots and different disturbances. Therefore, if there are control faults at the dynamic level, the kinematic control may be unstable.

Moreover, as indicated in most literatures, sliding mode control, which benefits from quick reaction, less information, and robustness to system uncertainties and external disturbances, is far more ideal for controlling mobile robotics such that lower the order of the systems and the systems are not regulated by the dynamics of the process, but rather by parameters chosen by the designer. Moreover, the dynamics of the sliding manifold can totally command the system performance once the sliding motion occurs**.**

1.3. General Objectives

The primary objective of this thesis is to model and design a global fast terminal sliding mode controller with quick reaching for tracking control differential drive mobile robot system.

1.3.1. Specific Objectives

Specifically, the core objectives of the research are:

- Developing the kinematics model of differential drive mobile robot
- Developing dynamic of differential drive mobile robot using langrage formulation
- Design a kinematic global fast terminal sliding control system for both angular and posture error to comes to zero in a finite time
- Design dynamic global fast terminal sliding mode controller with quick reaching for angular position error of each wheels to come to zero in a finite time
- Simulate and analyze dynamics of DDMR on MATLAB/SIMULINK
- Simulate the control algorithms on MATLAB/SIMULINK

1.4. Significant of the Research

Presently, Ethiopians don't pay much attention to the use of mobile robots in a variety of applications. This is mostly because such robots are seen in the country as a luxury good with no useful use. However, in situations like welding work, painting, and agricultural settings where safety, a lot of effort, efficiency, and precision are crucial, smart robots are needed to automate similar tasks. In order to meet the needs for safety, a substantial quantity of labor, efficiency, and precision in this situation, mobile robotics fills the gap. Modern technology, such weed-spraying, harvesting, and seed-planting vehicles, as well as inspection robots, may considerably boost agricultural output. Furthermore, by building the foundation for upcoming researchers and students to learn from and be inspired, the university will start to establish itself as one of the recently founded technical research institutes.

1.5. Methodology

To meet the objectives of the thesis, the following methods will be applied.

Literature review: in this part, the review of the differential drive mobile robot control techniques will be discussed with respect this work.

Dynamic modelling of DDMR: under this section, dynamic modelling of differential drive mobile robot derived using langrage formulation including model uncertainty.

Controller design: after dynamic model of DDMR has been obtained the next part will be SMC controller design for motion control system.

Simulation and control algorithm testing on MATLAB/SIMULINK: in this step, simulation result of controller test against both disturbances. If the controller design doesn't meet the expected output, controller parameters changed appropriately in order to meet objectives addressed.

Documentation and presentation: finally, research report will have concluded with results and summarized and final documentation will be presented according schedules.

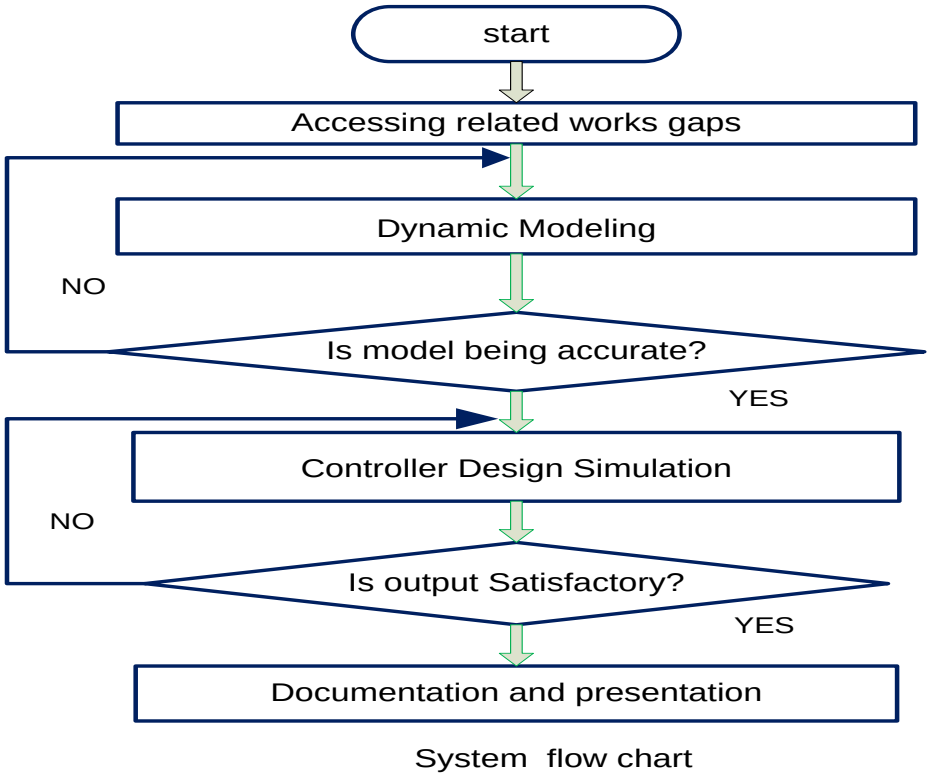

Figure 1: system flowchart

1.6. Limitation of thesis

One of the key factors preventing the practical realization of this was the absence of suitable materials for hardware implementation. Particularly, feedback sensors are challenging to obtain from domestic markets since they are perceived as luxury items, and no one will pay attention to such study fields. Moreover, due to a lack of time, this sector in particular needs enough time for future research into improved control systems for comparison with controllers for dedicated mobile robots.

1.7. Scope and expected outcomes

In this thesis report, modelling using langrage approach is employed and sliding mode trajectory tracking motion control system designed for differential drive mobile robot under both model uncertainty and external disturbances. Moreover, the scope of this thesis report is starting from

deriving dynamic modeling of a mobile robot and analysis dynamics of DDMR on MATLAB/Simulink and designing for trajectory tracking control, a sliding mode control system and testing algorithm on MATLAB/SIMULINK. The expected outcomes of this thesis are controller proposed in this thesis report will able improve the motion control system in all perspectives for dedicated mobile robot under both internal and external disturbances with a fast finite time convergence, high accuracy and significant reduction of chattering problems by including dynamic model of mobile robots in controller design.

1.8. Research Report Outline

The rest of the thesis is organized as follows.

In **chapter two,** DDMR related work, theory with respect SMC will be discussed. In chapter three, mathematical model of DDMR is presented with model uncertainty after that, controller is designed for system under chapter four. Depending on the designed controller simulation result and analysis is conducted in chapter five with simulation conducted on MATLAB/SIMULINK. Finally, conclusions and recommendations are drawn in chapter six.

CHAPTER TWO
RELATED TO WORKS AND THEORETICAL OVERVIEWS

2.1. Related works

This chapter discusses the review of literatures that have already been reported by various scholars. Assuming that a path planner is used to create the path. The goal of the trajectory tracking controller is to steer mobile robots along a predetermined path by modulating their angular and linear velocities. The key issue is how to properly regulate robot movement while tracking a specific trajectory. In recent years, there has been a lot of effort in the field of path tracking studies. Many different forms of nonlinear trajectory tracking controllers have been proposed in the literature for the trajectory tracking of such robots, and much has been published on how to solve the problem of motion under non-holonomic restrictions. In [6], a navigation system slide mode control was proposed for a mobile robot, but in this paper, the influence of dynamics of the mobile robot is not well thought-out and only steering system (kinematic problem) controller was designed. The authors in [7] introduced a back stepping controller for a Wheeled Mobile Robot. The kinematic control unit's job was to provide velocity outputs to the robot, which assisted to keep posture mistakes to a minimum. The response, on the other hand, was slow. Due to the large amount of difficult computations, the control has a reduced reaction time [8], In this study, the aim is to control a differential drive mobile robot (DDMR) to reach a target position despite the presence of disturbances, based on dynamic model of DDMR, a fuzzy target reaching control (FTRC) is proposed to achieve the target-reaching. [9] developed a PID-based cascaded control system that is master feedback kinematic and slave feedback dynamics based, with the translational velocity held constant and just the robot's rotating velocity controlled, resulting in a reduced response time. The paper proposed in [10], traditional sliding mode control system depending Gao's reaching methods implemented for mobile robot and fuzzy kinematic controller with dynamic proportional integral control is designed for mobile robot in [11], but finite time convergence main problems. Type two adaptive Proportional derivative controller (PID) Controller for DDMR [12]. This paper studies the effect of a fuzzy adaptive PID controller on the performance of a mechatronics system such as differential mobile robot. The proposed controller performance specification is compared by simulating the robot traveling an under no disturbance with circular and straight line reference trajectory. External disturbance is added later to the motor to for better comparisons between the two types of controllers. As we addressed in the above problems fuzzy logic control system always

prone to the problem of convergence due to computational difficulty results less reaction time. In the proposed adaptive fuzzy controller, fuzzy logic used to automatically tune PID controller gains. In [13], using forward kinematic current state of DDMR estimated and controller is designed base on inverse kinematics in this case, only kinematics controller designed using PI controller for go to go differential drive which lacks dynamic controller. in the last work dynamics of differential drive mobile robots. Moreover, summary the above literatures more elaborated in the table 2.1 for DDMR system modelling and control system.

Table 2. 1: literature gaps

Ref	Authors	Year	Focus	Gap
1	W. Benaziza, N. Slimane, and A. Mallem	2017	Terminal sliding mode control system	Only kinematic controller designed i.e. Dynamic of sliding mode control system ignored and chattering phenomena due to switching function
2	Muhammad Qomaruz Zaman; Hsiu-Ming Wu	2020	Fuzzy target reaching control for DDMR	Less reaction due to computational difficulty in fuzzy logic system
3	Vinod Raj N, Abraham T Mathew	2015	Cascaded master and slave PID controller for tracking control system	Used linear PID controller Actually mobile robot highly nonlinear system and coupled and it is not robust against external and internal disturbance and convergence and precision proposed controller also another problems
4	Navin Chandra P.; Mija S.J	2016	Robust controller for trajectory	Used conventional SMC and Poor convergence rate and poor efficiency in terms of

			tracking of a Mobile Robot	controller and finite time convergence and chattering problem also another problems
5	Thiago de A. Ushikoshi; Kamilla P. Peixoto; Filipe H. S. Souto; Thiago P. das Chagas; Leizer Schnitman	2018	Fuzzy master kinematic and Slave PID dynamic controller	Less convergence time due fuzzy master controller and linear PID for dynamic which is not robust which unable reject disturbances
6	Parham Dadash Pour; Khader M.J. Alsayegh; Mohammad A. Jaradat	2022	PID gain tuning type 2 fuzzy for DDMR motion control	Less reaction time which leads to poor convergence rate and traditional PID controller employed for motion of DDMR
7	Ravinder Singh; Gurpreet Singh; Vijay Kumar	2020	Control of closed-loop differential drive mobile robot using forward and reverse Kinematics	Classical goal to goal motion control using proportional controller which poor interims of convergence, robustness and accuracy of mobile robot motion regulation

2.2. Motion control for wheeled mobile robots

Firstly, the kinematic model usually considered for controller design, with the guess of perfect velocity tracking possible. The primary goal are identify appropriate velocity control of contributions that would alleviate the kinematic closed-loop control. Furthermore, unknown there are governor error at the dynamic level, the kinematic control will be unstable. As a result, control at the dynamic-level is at least as important as control at the kinematic level as shown in Fig. 2.1.

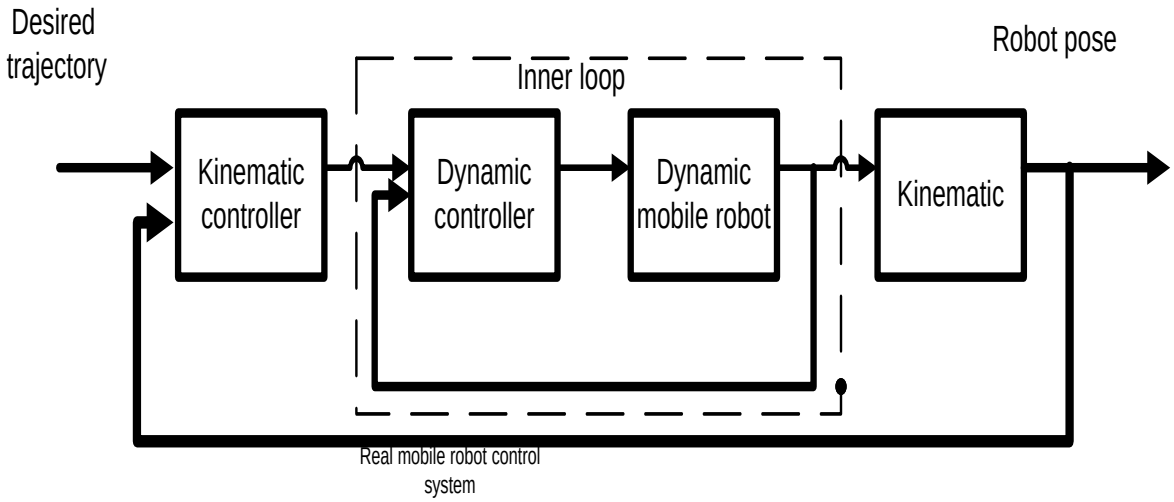

Figure 2. 1: real mobile control system

Motion control of WMR can be grouped in to the following types:

- Stabilizing point
- Trajectory tracking
- Path following

System stability can be considerably enhanced by using non-linear controllers as indicated in [14,15]. As soon as the vehicle has Non-holonomic constraints, point stabilization is a significant problem for control system designers because that objective cannot be achieved using smooth (or even continuous) state-feedback control rules, as stated in [16]. Smooth time-varying control laws [17, 18], as well as discontinuous and hybrid feedback laws [19, 20, 21], have all been used to solve this issue. For fully actuated systems, the trajectory tracking problem is well known, and suitable solutions may be found in advanced nonlinear control textbooks. However, research on under-actuated cars, or cars with fewer actuators than the state variables to be tracked, is still quite active. Lyapunov-based control rule [17], [24], as well as linearization and feedback linearization algorithms, have all been proposed.

2.3. Sliding mode in control design

Adjustable Construction Controller (VSC) is a type of control whose main objective is to move system states closer to a sliding surface. One of the most efficient methods for resolving control issues, sliding mode techniques are gaining popularity. Early in the 1950s in the Soviet Union, Emelyanov and a number of significant researchers—including Atkins and Itkis—developed and

elaborated VSC with SMC for the first time. Over the past ten years, VSC and SMC have drawn a lot of interest in the field of control research [25].

The most prominent characteristic of sliding mode control is its complete immunity to parametric uncertainty and outside disruption [26]. To push a nonlinear plant state trajectory onto a desirable and user-selected surface in the state space known as the slide or switching surface, and to retain it there for all subsequent time, VMC uses a high-speed switching control algorithm. This surface is known as the switching surface because a control path has one gain if the plant state trajectory is "above" the surface and a different gain if the trajectory is "below."

Through the process, the structure of control in the system changes from one to the next, giving rise to the term VSC. The control is same times known as SMC [26] to stress the importance of the sliding mode. The state trajectory's progression is separated in to two components.

- Reaching phase and
- Sliding phase

2.3.1. Sliding surface base approach

There are two types of sliding surfaces: linear and nonlinear. Here are several typical approaches for defining the sliding mode differential equation. Consider the following scenario.

$$x' = A(x) + B(x)u \; with \; sliding \; surface \; of \; s = \{x|s(x) = 0\} \quad (2.1)$$

Where $A(x), B(x)$ a functions of nonlinear control x and x $\in R^n$, u $\in R^m$.

1. *Canonic form:*

A form of controllable linear single input system is translated to canonic model system if the system is [28]:

$$x_i' = x_{i+1} \quad i = 1,2, \dots \dots \dots . n-1 \quad (2.2)$$

$$x_n' = -\sum_i^n a_i x_i + b.u \quad (2.3)$$

It is possible to define the sliding surface by:

$$s' = \frac{\partial s}{\partial x} s(x) = \lambda_1 x_1 + \lambda_2 x_2 + \cdots \dots . . + x_n = 0 \quad (2.4)$$

Where λ_1= constant, $i = 1,2, \dots, n-1$

Organize and conversion [29]: if the system (2.1) is lined and described as follow:.

$$x' = A(x) + B(x)u \quad (2.5)$$

Consider the case where Q is a non-singular Transformation.

$$BQ = \begin{pmatrix} 0 \\ B_2 \end{pmatrix} \tag{2.6}$$

Where is B_2 and nonsingular. After then, the system is turned into

$$x_1' = A_{11}x_1 + A_{12}x_2 \tag{2.7}$$

Where, $x_1 \in R^{n-m}$, $x_2 \in R^m$.

The switching surface can be expressed in the following way: $s(x) = \Delta_1 x_1 + \Delta_2 x_2$. We can assume, without losing generality, that Δ_2 is nonsingular, and we have a sliding mode $\Delta_1 x_1 + \Delta_2 x_2 = 0$, that is $x_2$is allied to the linarites to x_1 these condition as explain this formula:

$$x_1' = A_{11}x_1 + A_{12}x_2 \tag{2.8}$$
$$x_2' = -kx_1$$

Where, $k = \Delta_2^{-1}\Delta_1$. (2.8) represents an (n−m) the change of performance of the sliding mode is defined by the instruction system in x_1 is considered by way of the control input to the constrained system by:

$$x_1' = [A_{11} - A_{12}k]x_1 \tag{2.9}$$

The aforementioned procedures show how the challenging state feedback state design problem can be reduced to a reduced-order state feedback design challenge. It is possible to compute K using common feedback design techniques like pole appointment otherwise linear quadratic procedures since, in over-all, if (A, B) is controlled$A_{11_{,,}}$ A_{12}s likewise controllable. $[A_{11} - A_{12}k]$ Possesses desirable features after determining K, the desired switching function can be designed as follows:

$$(x) = \Delta_2[k, I].x \tag{2.10}$$

Where $\Delta 2$ tin to be designated subjectively. A simple selection is to let $\Delta 2 = I$.

2. The linear-quadratic (LQ) method

Intended for linear time-invariant systems, the optimum slipping method, or additional indeed, the ideal selection of the vector K of (2.9), can be discovered by minimizing a quadratic cost over an infinite time period [29]. For instance, LQ optimization can be used to find the ideal sliding mode for (2.9) by reducing its size because x2 is the system's input (2.9).

$$J = \int_{ts}^{\infty}(x_1^T Q_{11} + x_1 + 2x_1^T Q_{12}x_2 + x_2^T Q_{22}x_2)dt \tag{2.11}$$

We can let, without sacrificing generality$Q12 = 0$ and then the control optimal control x_2 is obtained by

$$x_2 = -Q_{22}^{-1}A_{12}^T P x_1 = -kx_1 \tag{2.12}$$

P is matrix of positive definite the Riccati equation's problem are:

$$A_{11}^T P + pA_{11} - pA_{12}Q_{22}^{-1}A_{12}^T p = -Q_{11} \tag{2.13}$$

The switching function (2.10) is then calculated by:

$$s(x) = kx_1 + x_2 = -[Q_{22}^{-1}A_{12}^T P].\, x \tag{2.14}$$

3. Time-varying surface for tracking control

One method is to express the descending surface according to the desired control bandwidth for a single input system.

$$s(x,t) = \left(\lambda + \frac{d}{dt}\right)^{n-1} x = 0 \tag{2.15}$$

The tracking error is denoted by the letter x and the closed –loop bandwidth is determined by λ which is a strictly positive constant. We can see that S is solely determined by the tracking error$X$.. For instance, if $if\ n = 2$

$$s = x' + \lambda x \tag{2.16}$$

Which is just a weighted combination of the location and errors velocity; and if $n = 3$

$$s = x'' + 2\,\lambda x' + \lambda^2 x \tag{2.17}$$

The scalar s can also be viewed to reflect a real quantity of chasing performance [30], [31].

Method of corresponding control, Recognize that there is an analogous control that t $s'(x) = 0$ is a essential ailment for the state trajectory to persist on the sliding surface $s(x) = 0$ [32] .

As a result, the setting$s'(x) = 0$, i.e

$$s' = \frac{\partial s}{\partial x}\, x' = \frac{\partial s}{\partial x}\left(A(x) + B(x)u(t)_{eq}\right) = 0 \tag{2.18}$$

Solving (2.18), for $u(t)$ eq. yields the equivalent control.

$$u(t)_{eq} = -\frac{\partial s}{\partial x}A(x)\left(\frac{\partial s}{\partial x}B(x)\right)^{-1} \tag{2.19}$$

Where, $\frac{\partial s}{\partial x}B(x)\ is$ nonsingular,

The dynamic of system governed by:

$$x' = \left(I - B(x)\left(\frac{\partial s}{\partial x}B(x)\right)^{-1}\frac{\partial s}{\partial x}\right)A(x) \tag{2.20}$$

4. Terminal sliding mode control

Selecting a switching manifold with the necessary dynamic for the state variables limited to the manifold is the aim of the sliding mode control design. Error dynamics, on the other hand, cannot converge to zero in a finite amount of time for conventional switching manifolds since they are

often linear hyper planes with asymptotic stability. Faster error convergence can be achieved by adjusting the sliding mode settings, but doing so will increase the control gain, which could lead to severe chattering on the sliding surface and lower system performance. When compared to the SMC design mentioned above, one of the most significant advantages of the terminal sliding mode (TSM) concept is announcing finite-time convergence to the sliding phase to complete the global finite-time convergence. The TSM control is established created on finite-time control concept [34,35] to realize the high convergence in the sliding of phase.

Further, high precision control was obtained using terminal SMC techniques.

The basic idea behind TSM control can be summed up as follows: Think about a second-order uncertain nonlinear dynamic system.

$$x'_1 = x_2 \tag{2.21}$$

$$x'_2 = f(x) + g(x) + b(x)u$$

Where,$x = [x_1, x_2]^T$ is the system state vector, $f(x)\ and\ b(x) \neq 0$ are a smooth nonlinear function of x and $g(x)$ symbolizes the unpredictability's and disruptions that must be satisfying $\|g(x)\| \leq l_g$ed.where, $l_g > 0$ and the scalar control input is u. The following first-order terminal sliding variable describes the standard TSM:

$$s = x_2 + \beta x_1^{\,q/p} \tag{2.22}$$

Where, $\beta > 0$ is a design constant, and p and q are positive odd integers that satisfy the following condition: $p > q$ The existence of TSM is a sufficient requirement.

$$\frac{1}{2}\frac{d}{dt}s^2 \leq \mu|s| \tag{2.23}$$

Where $\mu > 0$ is constant. For the system in equation (2.20) and (2.21) the following is an example of a common control design.

$$u = -b(x)^{-1}(f(x) + \beta\, {}^{q}\!/_{p}\, x_1^{\,{}^{p}\!/_{q}-1} x_2 + (l_g + \mu)sign(s) \tag{2.24}$$

Terminal Sliding Mode is ensured as a result of this:

It is clear that if$s(x) \neq 0$, the system states will reach the sliding mode s = 0 within the finite time t_r, which satisfies

$$t_r \leq \frac{|s(0)|}{\mu} \tag{2.25}$$

When the sliding mode s = 0 is attained, the following nonlinear differential equation describes the dynamics of the system:

$$x_2 + \beta {x_1}^{p/q} = 0 \tag{2.26}$$

the finite time t_s that is taken to travel from $x_1(t_r) \neq 0$ to $x_1(t_r + t_s) = 0$ is given by

$$t_s = \frac{p}{\beta(p-q)} |x_1(t_r)|^{1-\frac{q}{p}} \tag{2.27}$$

This suggests that both the system states x_1 and x_2 in the TSM manifold (2.27) converge to zero in finite time.

5. Global fast terminal sliding mode control

Asymptotical convergence of states is overcome by the standard sliding mode. Compared to traditional sliding mode control, fast terminal sliding mode control has a higher convergent characteristic. Additionally, the chattering phenomenon is avoided since the global rapid terminal sliding mode control lacks a switch function [36].

A new global fast terminal sliding surface is presented based on the linear and terminal sliding surfaces:

$$s = x' + \alpha x + \beta {x}^{q/P} \tag{2.28}$$

Where, x∈ R is stating, α, β>0, p and q (p>q) are positive odd numbers [36].

The time interval that the initial state x (0) ≠ 0 attains at x=0 is

$$t_s = \frac{p}{\alpha(p-q)} \ln \frac{\alpha x(0)^{(p-q)/p} + \beta}{\beta} \tag{2.29}$$

By designing α, β, p, q. In a finite amount of time, we can bring the system state to a condition of equilibriumt_s.

From equation (2.28) we have:

$$x' = -\alpha x - \beta {x}^{p/q} \tag{2. 30}$$

When the state *x* is far away from the origin, the fast terminal attractor determines the convergence time $x' = -\beta {x}^{p/q}$; when the state *x* approaches the origin *x* = 0, then, the convergent time is decided by the equation $x' = -\alpha x$. *x* converges to 0 Exponentially. As a result, the sliding surface's equation (2.29) is modified to include the terminal attractor, which causes the state to converge to zero in a finite amount of time. Additionally, the speed of the linear sliding surface is guaranteed. Therefore, the state is able to.

6. The global Sliding Surface Based Approach.

Mostly, the international dissolute of the terminal sliding mode surface can be considered as follows:

$$so = \dot{x} + \alpha x + \beta |x|^{\delta} \, sign\,(x) \tag{2.31}$$

$$\text{Where: } \alpha > 0, \beta > 0, 0 < \delta < 1. \tag{2.32}$$

For equation (2.32), when $so = 0$, the equation of sliding motion can be given by:

$$\dot{x} = -\alpha x - \beta |x|^{\delta} sign(x) \tag{2.33}$$

The first term of (2.33) is crucial when x is distant from 0. The moment equation (2.33) is crucial when x is near to 0. The performance of the global rapid terminal sliding mode is further improved by the proposed improved sliding surface in this section. A global fast terminal sliding mode manifold proposed as follows is motivated by the work in [44]: $s = \dot{x} + \frac{2\alpha}{1+e^{-\eta_1(|x|-e)}} x +$

$\frac{2\beta}{1+e^{\eta_2(|x|-e)}} |x|^{\delta} sign(x)$ (2.34)

Where $\alpha, \beta, \eta 1, \eta^2 > 0, 0 < \delta < 1, and\ \varepsilon = \left(\frac{\beta}{\alpha}\right) 1/(1-\delta)$ (2.35)

Choose a Lyapunov function$v_{3=0.5^2}$, then the time derivation v_3 is: When $s = 0$, the equation of SM can be described as:

$$\dot{x} = -\frac{2\alpha}{1+e^{-\eta 1(|x|-g)}} x - \frac{2\beta}{1+e^{\eta 2(|x|-g}} |x|^{\delta} sign(x) \tag{2.36}$$

$$\dot{v_3} x\dot{x} = -\frac{2\alpha}{1+e^{-\eta 1(|x|-e)}} \mathrm{x}^2 - \frac{2\beta}{1+e^{n2(|x|-\varepsilon}} |x|^{\delta} + 1 < 0 \tag{2.37}$$

It can be seen that $v3 > 0$ and $\dot{v}3 < 0$. Hence, state variables $X$and $\dot{x}$ container to be alleviated to the equilibrium point. Like to the reaching signal, at that time $|x(0)| > \varepsilon$, the sliding motion is also divided in to two stages:$x(0) \to |x| = \varepsilon$ and$|x| = \to x = 0$.

Stage 1:$x(0) \to |x| = \varepsilon$. Then first term of equation (4.24) plays a major role:

$$\int_0^{t3} dt = \int_g^{x(0)} \frac{1}{\frac{2\alpha}{\frac{1}{1+e^{-\eta 1(|x|-g}}|x| + \frac{2\beta}{1+e^{\eta 2(|x|-g_)}}|x|^{\delta}}} d\,(|x|) < \int_g^{x(0)} \frac{1}{\alpha|x|} d(|x|) = \frac{In(|x(0)|) - In(\varepsilon)}{\alpha} \tag{2.38}$$

Stage 2:$|x| = \varepsilon \to x = 0$. The second term of equation (2.37) plays a major role:

$$\int_0^{t4} dt = \int_0^{g} \frac{1}{\frac{2\alpha}{1+e^{-\eta 1(|x|-\varepsilon}}|x| + \frac{2\beta}{1+e^{\eta 2(|x|-\varepsilon}}|x|^{\delta}} d(|x|) < \int_0^{\varepsilon} \frac{1}{\beta|x|\delta} d(|x|) = \frac{1}{\beta(1-\delta)} \left|\varepsilon 1^{-\delta}\right| \tag{2.39}$$

Consequently, the amount of time of the sliding motion can be deliberated as:

$$ts = t3 + t4 < \frac{In(|x(0)| - In(\varepsilon)}{\alpha} + \frac{1}{\beta(1-\delta} |\varepsilon| 1^{-\delta} \quad (2.40)$$

In order to enhance the dynamic performance and quick convergence of Sliding Mode Control (SMC) and Terminal SMC (TSMC), which also achieves a finite-time convergence, the global fast terminal sliding mode surface is first proposed. An operator is then created using the suggested sliding surface utilizing the High-Order and Back stepping Control The controller offers smooth control torque, little position and velocity control faults, and less oscillation [46].

The Lagrange technique was initially used to create the dynamic model, of its zero-state response and 0% input reaction. Then, a series of balancing equations were. Derived using the Lyapunov method and the kinetic model carried performed to gauge its controllability and stability. Finally, It was possible to obtain the linear model of the robot in equilibrium [47]. The interactive model this work establishes a two-wheeled self-balancing robot operating in a slope environment, analyzes its controllability, and designs a GFTSMC controller.

2.3.2. Reaching law

In order to do this, choose a state feedback control role ($u = R^n, R^m$) that can propel the state trajectory in that direction and maintain it there. In other words, the managed system has to satisfy the achieving requirements. In general, Multi input and multi output systems, altered transferring strategies use different reaching rules during the approach to the sliding mode. The most often applied reaching laws and suggested control strategies are described in [37] and [38].

- The direct switching approach
- Approach based on the lyapunov function
- Gao strategy to enacting legislation

1. *The method of using a direct switching function is as follows:*

The classic enough situation for the appearance of sliding mode is to meet the criteria.

$$s_i' s_i < 0, i = 1, \ldots \ldots m$$

a similar approach or condition is proposed in [28], i.e.

$$\lim_{s_i \to 0^+} s_i' < 0 \; and \; \lim_{s_i \to 0^-} s_i' > 0$$

Distinct switching surfaces besides their intersections remain all sliding surfaces as a result of these reaching principles in a VSC. This reaching is global, but there is no assurance that it will take a certain amount of time.

2. *The technique based on the Lyapunov function:*

Selecting and developing a stabilizing control law is necessary to maintain the system states on such a surface. The generalized version of the equation below was proposed by Stoline and Li in [26] for selecting the shape of the sliding surface. Where x, the control variable or state vector, t(x), the tracking error defined as x d-x, x, a positive constant interpreting the surface dynamics, and f, the relative degree of the sliding mode controller are present. When the state trajectory hits the sliding surface, this is the attractiveness condition. The equation below illustrates how to construct the Lyapunov candidate function, a positive scalar function.

Select the control law that will cause the system state variables' reduction of this function: Although there is no set method for choosing a Lyapunov function, in this case you should look at the positive candidate Lyapunov function for all single dynamics systems. Choose the $u(t)_c$ for negative definite of $v(x,t)' < 0$ so that the trajectory converge to the surface, typical choice$u(t)_c = u(x)sign(s)$, where, $(x)\epsilon R^{mxm}$.

Although locations on discrete transferring surfaces may or may not fit to the sliding surface, this getting law creates a VSC in which the ultimate sliding mode is only guaranteed at the intersection of all switching surfaces.

3. *GAO's reaching law approach:*

In [39], GAO and Hung planned a reaching law that uses a differential equation to directly specify the dynamics of the switching surface.

Reaching phase and sliding phase are both part of the sliding mode based on the accomplishment rule. The sliding phase drive system ensures slide to equilibrium, while the reaching phase drive system maintains a steady manifold. The switching variable s(x) to reach the switching manifold S at a consistent rate by this law $|s'_i| = -q_i$. The simplicity of this reaching law is its greatest asset. However, if qi is too small, the reaching time will be excessively long. A huge qi, on the other hand, will produce severe chattering.

4. *Attaining a constant plus proportionate rate:* $s' = -\mathrm{Q}\,\mathrm{sign}(\mathrm{s}) - \mathrm{P}.\mathrm{s}.$

When s is big, introducing the proportional rate term –ps, forces the state to approach the switching manifolds faster.

5. *Power rate reaching:* $s' = -p_i|s_i|^{\alpha}\mathrm{sign}(s_i), 0 < \alpha < 1, \mathrm{i} = 1, \ldots\ldots\ldots, \mathrm{m}$

Once the state is far-off a forms to the switching assorted, this reaching rule raises the rate, but when the state is close to the manifold, it decreases the rate.

6. Quick Reaching Law Base Approach

The study simultaneously suggests a novel sliding surface and a novel reaching law.

Since the rapid influence reaching rule and the dual power reaching rule are combined, the suggested attainment law with dual variable power relations has a high capacity for adaptation. It may result in system states approaching the sliding surface closer or farther away more quickly. Thanks to the improved global rapid terminal sliding mode surface with dynamic coefficient scan, the system approaches the equilibrium point with a faster convergence rate. The proposed reaching law and sliding surface are combined to produce a revolutionary global fast terminal sliding mode controller. The dynamic reaction rate of the system can be greatly increased with this controller. The control approach may also produce strong control performance and minimal chattering. Additionally, three experiments validate and enhance its quality. The proposed reaching law and sliding surface alone can be used to generate various sliding mode controllers.

The suggested control mechanism can also be used to manage higher-order systems. Additionally, the high-order systems that demand additional research utilize the novel global fast terminal sliding mode controller's architecture [44]. The double power reaching law and the rapid power reaching law can generally be expressed individually as follows:

$$\dot{s} = -K_1|s|^{r1}\sin(s) - K_2 s \tag{2.41}$$

$$\dot{s} = -K_1|s|^{r1} sign(\mathrm{s})\,|s|^{r2}\sin(s) \tag{2.42}$$

Where$K_1 > 0, K_2 > 0, 0 < r^1 < 1, r^2 > 1$ When the system is removed from the sliding surface, or when |s|>1, (2) moves more quickly than (1). However, |s|<1, (2.41) has a quicker speed when the system state is close to the sliding surface (2.42). Combining the benefits of the two previous quick reaching laws, the following new law is suggested:

$$\dot{s} = -K_1|s|^{g1} sign(s) - K_2|s|^{g2} sign(s) \tag{2.43}$$

With: $g1 = fo + f1\tanh(s) - f2\tanh(\lambda s2)$

$$g2(s) = \begin{cases} g, if|s| \geq 1 \\ g, if|s| < 1 \end{cases} \quad (2.44)$$

Where $k_1, k_2, \lambda > 0, 0 < f2 < fo < 1, f1 > 1, g = fo + f1 - f21, and\ r$ is positive even number:

Strong adaptability is present in the innovative reaching law with two variable power terms. Equation (3) is identical to the following phrase: g2(s) Piecewise function by design appropriate parameter r and λ.

$$\begin{cases} \dot{s} = -k_1|s|g\ sign(s) - k_2|s|g\ sign(s), & |s| \geq 1 \\ \dot{s} = -k_1|s|fo - f2\ \ sign(s) - k_2 s, & 0 < |s| < 1 \\ \dot{s} = -k_1|s|fo\ sign\ (s) - k_2 s, & near|s| = 0 \end{cases} \quad (2.45)$$

When |s|<=1, both terms participate in the process, making (3) more rapidly reachable than the double authority success law. The realization is to changes from a double high reaching law to a quick control reaching law when $0 < |s < 1|$and has a faster reaching rate. It is important to keep in mind that |s|fo<|s|fo-f2 can accomplish the desired chattering decrease when the adjustable s is near to 0. Thus, that is the system is far from or close to a sliding surface, the innovative reaching law can both eliminate chattering and have quick convergence.

2.4 Summary of literature review

The thesis mentioned above mainly have to do with various models, motion control techniques, and theories of control. This thesis is addressing trajectory control techniques, including kinematic control and dynamic controller, robustness to internal and external disturbances, convergence rate, finite time convergence, control system accuracy, modeling, and chattering problem are therefore presented as in table 2.1 above. A finite time global fast terminal sliding control system with quick reaching approaches was used in the thesis report to fill in any gaps connected to the aforementioned issues. This system will have high precision, rapid convergence, and a significant reduction in chattering phenomena.

CHAPTER THREE
MATHEMATICAL MODELING

3.1. System description

Differential drive robot is a two-degrees-of-freedom robots that contains two motors drive the two front wheels, while the second castor wheel serves as a guiding and stabilizing wheel. The world coordinate I = (x, y,θ), and B is the middle point of mobile robot. The main parameters are as follows,

- As indicated in Fig.3.1, R is the radius of driving wheels', D is the distance from the center of the mobile robot center and its driving wheels, and an is the distance between the mass center and the MP's rotating center.
- Consider the WMM in Fig.3.1 below, its model is based on the following expectation: Two driving wheels on an axis that goes through the geometric center of the mobile robots regulate the DDMR body motion.

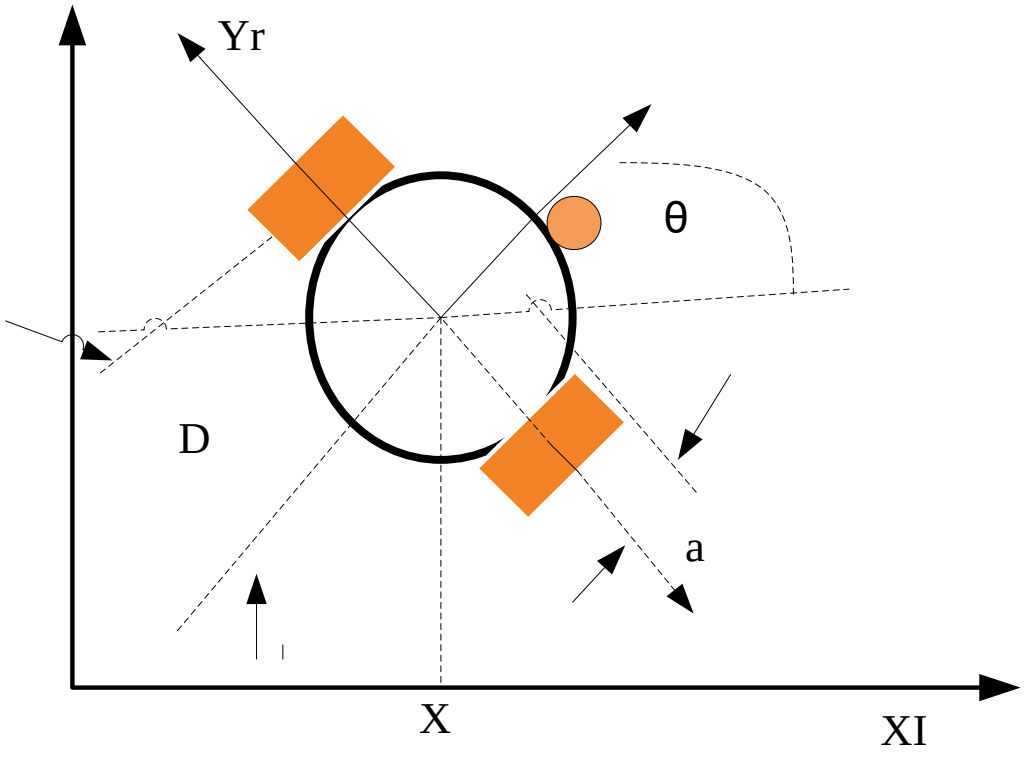

Figure 3. 1: Frame and variable description of DDMR

3.2. Kinematic and dynamic modeling of DDMR

Wheeled mobile robots are a type of non-holonomic machine that can navigate and perform tasks autonomously. The peculiar characteristic of such a system is that they can't move sideways due to the perfect rolling without slipping constraints of their wheels. In this section, we are going to explore this behavior briefly to the unicycle [43].

3.2.1. Kinematic differential drive wheeled mobile robot platform

Kinematic modeling is the study of mechanical system motion without taking into account the factors that influence the motion [43]. The major goal of kinematic modeling for the DDMR is to depict the robot velocities as a function of the driving wheels' velocities and the robots geometric attributes [43]. Two different coordinate system (frames) must be defined to characterize the WMR's position in his environment.

System of Inertial/world Coordinate: This frame is also known as the reference frame and is denoted by the letters {XI, YI}. *The Robot Coordinate System:* is a local frame that is attached to the WMR and consequently moves with it. {Xr, Yr} is the symbol for this frame.

A mechanical system is subjected to two constraints holonomic and Nonholonomic constraints [43]. Holonomic constraints: are restrictions on the location (configuration) of a system of particles. All holonomic constraints can be transformed into constraint integration constants.

Non-holonomic constraints: Constraints that limit particle velocities but not their positions, with at least one nonintegrable (i.e. non-holonomic) constraint.

Two non-holonomic constraint equations describe the motion of a DDMR:

No lateral slip motion: the robot can only move in one direction (forward and backward) or in the same direction as the wheel's plane of rotation, but not sideways, as shown in Fig 3.2

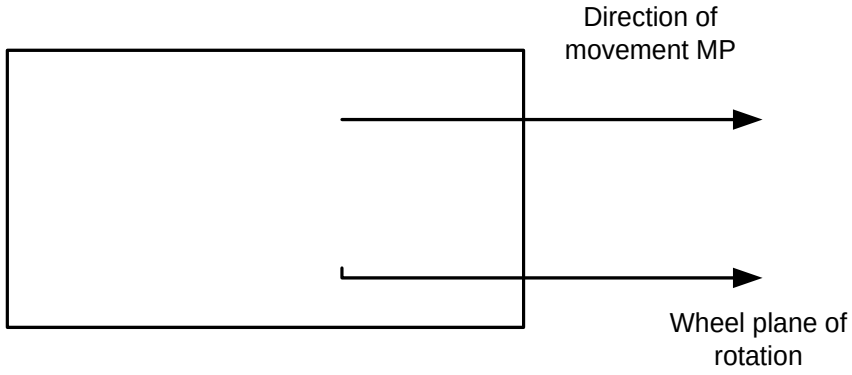

Figure 3. 2 No Lateral slip due to the same in robot motion direction and plane of rotation of wheels.

$$y_r' = 0 \tag{3.1}$$

The velocity in the inertial frame is calculated using the orthogonal rotation matrix T (θ),

$$cos\theta y_c' - sin\theta x_c' = 0 \tag{3.2}$$

Pure rolling constraint:

Longitudinal slip happens when 100% of the applied torque is communicated to the ground, moving the wheel forward as a result of the input torque.

The relationship between the wheel velocities and the linear velocities of the robot frame is as follows:

$$v_{pr} = r\phi_r' \tag{3.3}$$

$$v_{pl} = r\phi_l' \tag{3.4}$$

The robot's position in the Xr is always zero since the coordinate system is fixed on the robot $\varepsilon = [x, y, \theta]^T$ of the robot in the XI frame.

It can be found from Fig 3.1, above that

$$x_i' = cos\theta x_r' - sin\theta y_r' \tag{3.5}$$

$$y_i' = sin\theta x_r' + cos\theta y_r' \tag{3.6}$$

Since, both the world and robot frame are share the same z-axis, we can write:

$$\theta_i' = \theta_r' \tag{3.7}$$

It's possible to conveniently write combining the above equation (3.5), (3.6), and (3.7),

$$\varepsilon_i' = T(\theta)\varepsilon_r' \tag{3.8}$$

Where $T(\theta) = \begin{pmatrix} cos\theta & -sin\theta & 0 \\ sin\theta & cos\theta & 0 \\ 0 & 0 & 1 \end{pmatrix}$

The task now is to find the speed of the robot in its frame, where we use kinematic constraints of individual wheels. As a result, we may calculate the wheel x' forward speed as:

$$x_r' = r\phi' \tag{3.9}$$

Where ϕ is the encoder rotational position reading, ϕ' is the driving wheel's radius, and r is the rotational speed.

It's critical to calculate the contribution of each wheel separately, assuming that the other wheels aren't activated. The distance traveled by the center point is exactly half of the distance traveled by each wheel, assuming the non-actuated wheel rotates around its ground contact point. That is,

$$x_r' = \frac{r\phi_r'}{2} - \frac{r\phi_l'}{2} \tag{3.10}$$

Given the speeds of the right and the left wheels, ϕ_r' *and* ϕ_l', respectively.

The typical wheel restriction tells us that the robot can never slide, hence the robot's y-axis always zeros i.e. $y_r' = 0$.Rotation about the z-axis is achieved by imagining the robot's wheel spinning in opposite directions.

Given an axle diameter (distance between the robot's wheels) D, we can have written as:

$$\theta_r' = \frac{r\phi_r'}{2D} - \frac{r\phi_l'}{2D} \tag{3.11}$$

In the inertial frame, the DDMR velocities can be calculated as follows:

$$\begin{pmatrix} x_i' \\ y_i' \\ \theta_i' \end{pmatrix} = \begin{pmatrix} cos\theta & -sin\theta & 0 \\ sin\theta & cos\theta & 0 \\ 0 & 0 & 1 \end{pmatrix} \left(\begin{pmatrix} \frac{r\phi_r'}{2} + \frac{r\phi_l'}{2} \\ 0 \\ \frac{r\phi_r'}{2D} - \frac{r\phi_l'}{2D} \end{pmatrix} \right) \tag{3.12}$$

It's convenient since the opinion of understanding of control system analysis and design to re-write the above equation (3.12),

$$\begin{pmatrix} x_i' \\ y_i' \\ \theta_i' \end{pmatrix} = \begin{pmatrix} \frac{rcos\theta}{2} & \frac{rcos\theta}{2} \\ \frac{rsin\theta}{2} & \frac{rsin\theta}{2} \\ \frac{r}{2D} & -\frac{r}{2D} \end{pmatrix} \begin{pmatrix} \phi_r' \\ \phi_l' \end{pmatrix} \tag{3.13}$$

The kinematic constraints (m=3) equations of the wheels can be written for the generalized coordinates of the platform being q=[x, y, θ, ϕ_r, ϕ_l]^T, we can expand the kinematic expression as

$$\begin{pmatrix} x_i' \\ y_i' \\ \theta_i' \\ \phi_r' \\ \phi_l' \end{pmatrix} = \begin{pmatrix} \frac{rcos\theta}{2} & \frac{rcos\theta}{2} \\ \frac{rsin\theta}{2} & \frac{rsin\theta}{2} \\ \frac{r}{2D} & -\frac{r}{2D} \\ 1 & 0 \\ 0 & 1 \end{pmatrix} \begin{pmatrix} \phi_r' \\ \phi_l' \end{pmatrix} \tag{3.14}$$

The kinematic formulation above will have to be modified if the mobile robot's center of mass and the center of its axle do not coincide, and the distance from the center of mass of its axle is defined as a. Accordingly, we take the succeeding kinematic equations (m=3) at the center of mass (x_c, y_c) of the robot:

$$\begin{cases} cos\theta y_c' - sin\theta x_c' - a\theta' = 0 \\ cos\theta x_c' + sin\theta y_c' + D\theta' - r\phi_r' = 0 \\ cos\theta x_c' + sin\theta y_c' - D\theta' - r\phi_l' = 0 \end{cases} \tag{3.15}$$

Using the already defined generalized coordinate vector $q=[x, y, \theta, \phi_r, \phi_l]^T$, of the robot, it's possible to write the above equation (3.15), these in matrix form as;

$$\begin{pmatrix} -sin\theta & cos\theta & -a & 0 & 0 \\ cos\theta & sin\theta & D & -r & 0 \\ cos\theta & sin\theta & -D & 0 & -r \end{pmatrix} \begin{pmatrix} x_i' \\ y_i' \\ \theta_i' \\ \phi_r' \\ \phi_l' \end{pmatrix} = 0 \tag{3.16}$$

Which is equivalent to the kinematic constraint of a non-holonomic system described above, i.e.

$$A^T(q)q' = 0 \tag{3.17}$$

It's possible to choose the vector of generalized velocity $q=[x, y, \theta, \phi_r, \phi_l]^T$ of the robot satisfying the constraint equation in:

$$\begin{pmatrix} x_i' \\ y_i' \\ \theta_i' \\ \phi_r' \\ \phi_l' \end{pmatrix} = \begin{pmatrix} \frac{r(Dcos\theta - asin\theta)}{2D} & \frac{r(Dcos\theta + asin\theta)}{2D} \\ \frac{r(Dsin\theta + acos\theta)}{2D} & \frac{r(Dsin\theta - acos\theta)}{2D} \\ \frac{r}{2D} & -\frac{r}{2D} \\ 1 & 0 \\ 0 & 1 \end{pmatrix} \begin{pmatrix} \phi_r' \\ \phi_l' \end{pmatrix} \tag{3.18}$$

The above equation (3.18) and equation (3.14) are identical provided that the center of mass of the whole robot and the center axle coincide i.e. a=0. Obtaining the right and left wheel angular speeds from wheel encoders, we can find the position and orientation of the robot by integrating the above equations.

3.2.2. Dynamic modeling of DDMR using Lagrange formulation

The Lagrangain formulation approach, which characterizes the behavior of a dynamic system in terms of work and energy stored in the system rather than forces and moments of the individual components involved, will be used to create the dynamic model of the mobile robot in the following sections [43]. We must now proceed by making use of the robot's schematic diagram, which is displayed in Fig. 3.1.The robot's parameters are described in the manner that follows.

R = Radius of the driving wheels

D= the distance between the robot's axle center and each of its driving wheels

A = the distance between a location on the robot's axle center and its center of mass

m_c = is the weight of the mobile robot, excluding the motor rotors and the driving wheels

m_w = the combined mass of each driving wheel's motor and its rotor.

I_c= The junction of the robot's Xr-axis and the driving wheel axis results in the moment of inertia of the mobile robot without driving wheels and the rotors of the motors about a vertical axis.

I_w = is the rotational inertia of the motor rotor and each driving wheel around the wheel axis.

I_w= the rotor's and each driving wheel's moment of inertia with respect to the wheel diameter.

We begin the formulation by defining the Lagrangain L of the mobile robot as the difference of between its kinetic energy T and potential energy U [43].

$$(q, q') = T(q, q') - U(q) = \frac{1}{2} q'^T B(q) q' - U(q) \tag{3.19}$$

The dynamic equations of the motion of the mobile robot are generated using Lagrangain formulations, and B(q) is a positive and symmetric definite matrix of the mechanical system as

$$\frac{d}{dt}\left(\frac{\partial L}{\partial q'}\right) - \left(\frac{\partial L}{\partial q}\right) = s(q) + A(q)\lambda \tag{3.20}$$

Where, s(q) represents an (n x m) matrix which maps the m=n-k external inputs τ to generalized forces that perform work on q, A(q) is a transpose of the (k x n) matrix of the kinematic constraints, and λ is a vector of Lagrangain multipliers, likewise $A(q)\lambda$ represents the vector of reaction forces at the generalized coordinate level.

At the center of mass of the platform, we compute the components of the speed of the robot as:

$$\theta' = \omega = \frac{r\phi_r'}{2D} - \frac{r\phi_l'}{2D} \tag{3.21}$$

Finding the kinetic and potential energy that govern the motion of the DDMR is the first step in deriving the dynamic model using the Lagrange technique. In addition, because the DDMR is travelling in the XI-YI plane, its potential energy is assumed to be zero. The total of the kinetic energies of the robot platform without wheels plus the kinetic energies of the wheels and actuators equals the DDMR's kinetic energies. The robot platform's kinetic energy is:

$$T_c = \frac{1}{2} m_c v_c^2 + \frac{1}{2} I_c \theta'^2 \tag{3.22}$$

While the right and left wheels' kinetic energy is,

$$T_{wr} = \frac{1}{2} m_w v_{wr}^2 + \frac{1}{2} I_m \theta'^2 + \frac{1}{2} I_w \phi_r'^2 \tag{3.23}$$

$$T_{wl} = \frac{1}{2} m_w v_{wl}^2 + \frac{1}{2} I_m \theta'^2 + \frac{1}{2} I_w \phi_l'^2 \tag{3.24}$$

All velocities will be defined as functions of the generalized coordinates using the general velocity equation in the inertial frame.

$$v_i^2 = x_i^2 + y_i^2 \tag{3.25}$$

In terms of generalized coordinates, the Xi and Yi components of the center of mass and wheels can be calculated as follow

$$\begin{cases} x_c = x_i + a\cos\theta \\ y_c = y_i + a\sin\theta \\ x_{wr} = x_i + D\sin\theta \\ y_{wr} = y_i + D\cos\theta \\ x_{wl} = x_i - D\sin\theta \\ y_{wl} = y_i + D\cos\theta \end{cases} \tag{3.26}$$

The system's kinetic energy is then conveniently started by combining equations (3.22), (3.23), (3.24), (3.25) and (3.26) as:

$$(q, q') = \frac{1}{2}m(x_i^2 + y_i^2) + m_c a\theta'(\cos\theta y_i' - \sin\theta x_i') + \frac{1}{2}I\theta'^2 + \frac{1}{2}I_w(\phi_r'^2 + \phi_l'^2) \tag{3.27}$$

The following new parameters are introduced in this section:

$$m = m_c + 2m_w$$

$$I = 2m_w D^2 + m_c a^2 + 2I_m + I_c$$

Finally, using the Lagrangain formulation provided in, the dynamic equations of motion for the mobile robot may be written,

$$\frac{d}{dt}\left(\frac{\partial T}{\partial q_i'}\right) - \left(\frac{\partial T}{\partial q_i}\right) = f_i - a_{1i}\lambda_1 - a_{2i}\lambda_2 - a_{3i}\lambda_3 \; for \; i = 1, \ldots 5 \tag{3.28}$$

For q is defined as generalized coordinates, f_i represents generalized forces, a_{ij} are components of the kinematics constraints $A^T(q)\; and\; \lambda$ are lagrangain multipliers [43].

From all of the preceding equations, we can get the following dynamic model for the mobile robot (3.26) and (3.28) as follows:

$$mx'' - m_c a\theta'^2\cos\theta - m_c a\theta''\sin\theta = -a_{11}\lambda_1 - a_{21}\lambda_2 - a_{31}\lambda_3 \tag{3.29}$$

$$my'' - m_c a\theta'^2\sin\theta - m_c a\theta''\cos\theta = -a_{12}\lambda_1 - a_{22}\lambda_2 - a_{32}\lambda_3 \tag{3.30}$$

$$m_c a(y''\cos\theta - x''\sin\theta) + I\theta'' = -a_{13}\lambda_1 - a_{23}\lambda_2 - a_{33}\lambda_3 \tag{3.31}$$

$$I_w\phi_r'' = \tau_r - a_{14}\lambda_1 - a_{24}\lambda_2 - a_{34}\lambda_3 \tag{3.32}$$

$$I_w\phi_l'' = \tau_l - a_{15}\lambda_1 - a_{25}\lambda_2 - a_{35}\lambda_3 \tag{3.33}$$

The factor a_{ij} are kinematics constraints of the robot defined as $A^T(q)$ i.e. $A(q) = \begin{pmatrix} -\sin\theta & \cos\theta & -a & 0 & 0 \\ \cos\theta & \sin\theta & D & -r & 0 \\ \cos\theta & \sin\theta & -D & 0 & -r \end{pmatrix}$

Therefore, our model reduces to the following equations:

$$mx'' - m_c a\theta'^2\cos\theta - m_c a\theta''\sin\theta = \lambda_1\sin\theta - (\lambda_2 + \lambda_3)\cos\theta \tag{3.34}$$

$$my'' - m_c a\theta'^2 sin\theta - m_c a\theta'' cos\theta = -\lambda_1 cos\theta - (\lambda_2 + \lambda_3)sin\theta \quad (3.35)$$

$$m_c a(y''cos\theta - x''sin\theta) + I\theta'' = a\lambda_1 + (\lambda_2 - \lambda_3)D \quad (3.36)$$

$$I_w \phi_r'' = \tau_r + r\lambda_2 \quad (3.37)$$

$$I_w \phi_l'' = \tau_l + r\lambda_3 \quad (3.38)$$

Where, τ_r and τ_l are right and left wheel motor torques.

The mobile robot dynamic model in the above form (3.34) to (3.38) equation can be rewritten in vector form for the convenience of control system analysis and design as follows:

$$M(q)q'' + c(q,q') = E(q)\tau - \quad A^T(q)\lambda \quad (3.39)$$

$$M(q) = \begin{pmatrix} m & 0 & -m_c asin\theta & 0 & 0 \\ 0 & m & m_c acos\theta & 0 & 0 \\ -m_c asin\theta & m_c acos\theta & I & 0 & 0 \\ 0 & 0 & 0 & I_w & 0 \\ 0 & 0 & 0 & 0 & I_w \end{pmatrix}, c(q,q^{\cdot}) = \begin{pmatrix} -m_c acos\theta \\ -m_c asin\theta \\ 0 \\ 0 \\ 0 \end{pmatrix},$$

$$E(q) = \begin{pmatrix} 0 & 0 \\ 0 & 0 \\ 0 & 0 \\ 1 & 0 \\ 0 & 1 \end{pmatrix}, \tau = \begin{pmatrix} \tau_r \\ \tau_l \end{pmatrix}, \lambda = \begin{pmatrix} \lambda_1 \\ \lambda_2 \\ \lambda_3 \end{pmatrix} \quad (3.39)$$

Where M (q) represents the inertia matrix of nxnsize, $c(q,q^{\cdot})$ denotes centripetal and Coriolis forces matrix, $E(q)$ is the input transformation matrix and τ is an input vector.

3.3. Representation of in state space.

It's imperative to write the dynamic and kinematic model equation of motion of the robot in a form easier and convenient for control system analysis and design. Here, we shall achieve this by employing the concept of state-space realization [43]. Firstly, let us recall the two input most important system equations of the differential drive wheeled mobile robot we developed above equations (3.14) and (3.39).

$$\begin{pmatrix} x_i' \\ y_i' \\ \theta_i' \\ \phi_r' \\ \phi_l' \end{pmatrix} = \begin{pmatrix} \frac{r(Dcos\theta - asin\theta)}{2D} & \frac{r(Dcos\theta + asin\theta)}{2D} \\ \frac{r(Dsin\theta + acos\theta)}{2D} & \frac{r(Dsin\theta - acos\theta)}{2D} \\ \frac{r}{2D} & -\frac{r}{2D} \\ 1 & 0 \\ 0 & 1 \end{pmatrix} \begin{pmatrix} \phi_r' \\ \phi_l' \end{pmatrix} \quad (3.40)$$

$$M(q)q'' + c(q,q') = E(q)\tau - \quad A^T(q)\lambda \quad (3.41)$$

Here let's put this differently i.e. in the kinematic model above, letting

$$(q) = \begin{pmatrix} \frac{r(D\cos\theta - a\sin\theta)}{2D} & \frac{r(D\cos\theta + a\sin\theta)}{2D} \\ \frac{r(D\sin\theta + a\cos\theta)}{2D} & \frac{r(D\sin\theta - a\cos\theta)}{2D} \\ \frac{r}{2D} & -\frac{r}{2D} \\ 1 & 0 \\ 0 & 1 \end{pmatrix}, and\ \eta = \begin{pmatrix} \phi_r' \\ \phi_l' \end{pmatrix} \quad (3.42)$$

This would give us the same model as above of:

$$q' = s(q)\eta \quad (3.43)$$

The transformation matrix S (q) is in the null space of the constraint matrix A (q) which maybe proven consequently, we have:

$$s^T(q)A^T(q) = 0 \quad (3.44)$$

The time derivative of equation (3.43) is thus given,

$$q'' = s'(q)\eta + \eta' s(q) \quad (3.45)$$

Equations (3.43) and (3.44) are substituted in the main equation (3.41), we obtain

$$(q)\big(s'(q)\eta + \eta' s(q)\big) + V(q,q')(s(q)\eta) = E(q)\tau - A^T(q)\lambda \quad (3.46)$$

Then, by reshuffling the balance (3.46) and multiplying both sides of $s^T(q)$ by, we get:

$$s^T(q)M(q)\big(s'(q)\eta)\big) + s^T(q)\big(M(q)\eta' s(q)\big) + V(q,q')(s(q)\eta) = s^T(q)E(q)\tau - s^T(q)A^T(q)\lambda \quad (3.47)$$

Where the final term from equation (3.47) is also zero. The new matrices are now being defined:

$$\bar{M}(q) = s^T(q)M(q)s(q) \quad (3.48)$$

$$\bar{V}(q) = s^T(q)M(q)s'(q) + s^T(q)V(q,q')s(q), and\ \bar{E}(q) = s^T(q)E(q) \quad (3.49)$$

The dynamic equations are simplified to the following form:

$$\bar{M}(q)\eta' + \bar{V}(q)\eta = \bar{E}(q)\tau \quad (3.50)$$

Where $\bar{M}(q) = \begin{pmatrix} I_w + \frac{r^2(mD^2+I)}{4D^2} & \frac{r^2(mD^2-I)}{4D^2} \\ \frac{r^2(mD^2-I)}{4D^2} & I_w + \frac{r^2(mD^2+I)}{4D^2} \end{pmatrix}$ (3.51)

$$V(q,q^{\cdot}) = \begin{pmatrix} 0 & \frac{r^2 m_c a\theta^{\cdot}}{2D} \\ -\frac{r^2 m_c a\theta^{\cdot}}{2D} & 0 \end{pmatrix} = \begin{bmatrix} V_{11} & V_{12} \\ V_{21} & V_{22} \end{bmatrix}, and\ \bar{E}(q) = \begin{pmatrix} 1 & 0 \\ 0 & 1 \end{pmatrix}$$

The DDMR's linear and angular velocities (v, w) can also be used to transform the equations of motion (3.50). It's easy to see how the model equations (3.50) can be reordered in the resulting as we compressed formula using the kinematic model equations (3.14).

$$\left(m + \frac{2I_w}{r^2}\right) v' - m_c\, a\omega^2 = \frac{(\tau_r + \tau_l)}{r} \tag{3.52}$$

$$\left(I + \frac{2I_w D^2}{r^2}\right) \omega' - m_c a\omega v = \frac{D(\tau_r - \tau_l)}{r} \tag{3.53}$$

CHAPTER FOUR
CONTROLLER DESIGN

4.1. Trajectory tracking control design for mobile platform

The DDMR system dynamics should be taken into account for good motion. Additionally, a genuine mobile robot control system is depicted in Fig. 4.1, which includes both inner and exterior controllers. As suggested in [13], the controller structure in this instance should be divided into two stages.

- Dynamic controller depending on the DDMR dynamics for velocity tracking
- kinematic level control, used to control both translational and rotational position of mobile robot

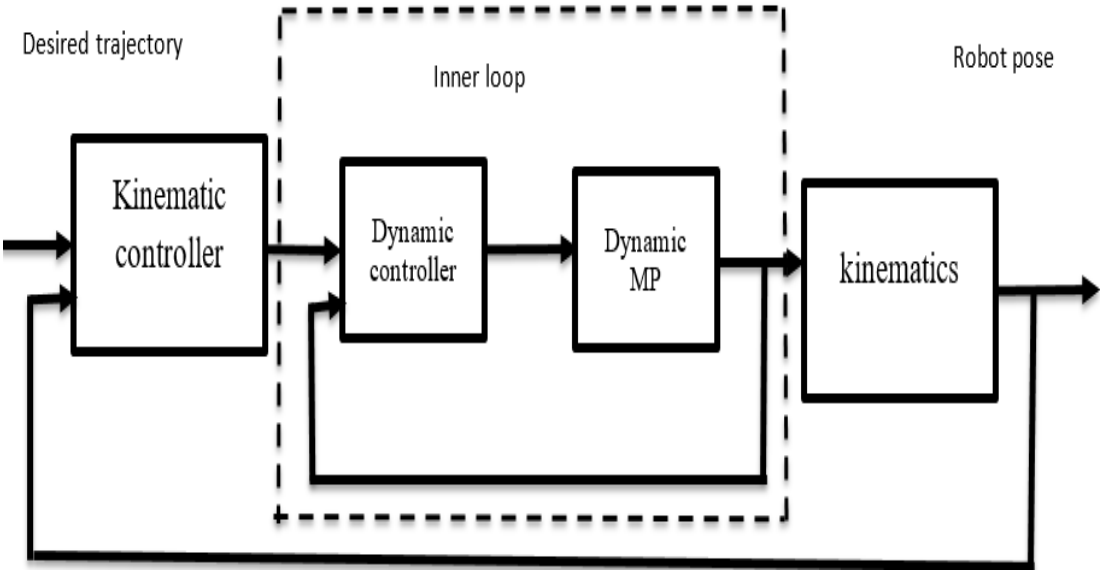

Figure 4. 1: Real mobile robot control system

4.1.1. Kinematic level Controller Design

The kinematic modelling from the equation (3.13) can be written as:

$$\begin{pmatrix} x' \\ y' \\ \theta' \end{pmatrix} = \begin{pmatrix} \cos\theta & 0 \\ \sin\theta & 0 \\ 0 & 1 \end{pmatrix} \begin{pmatrix} v \\ \omega \end{pmatrix} \tag{4.1}$$

Where v and ω are the linear velocities and angular velocities, with respectively with regard to the inertial basis frame. The mobile robot's movement begins at the position $p = (x, y, \theta)^T$ to desired position $p_d = (x_d, y_d, \theta_d)^T$ as shown in Fig. 4.2 below,

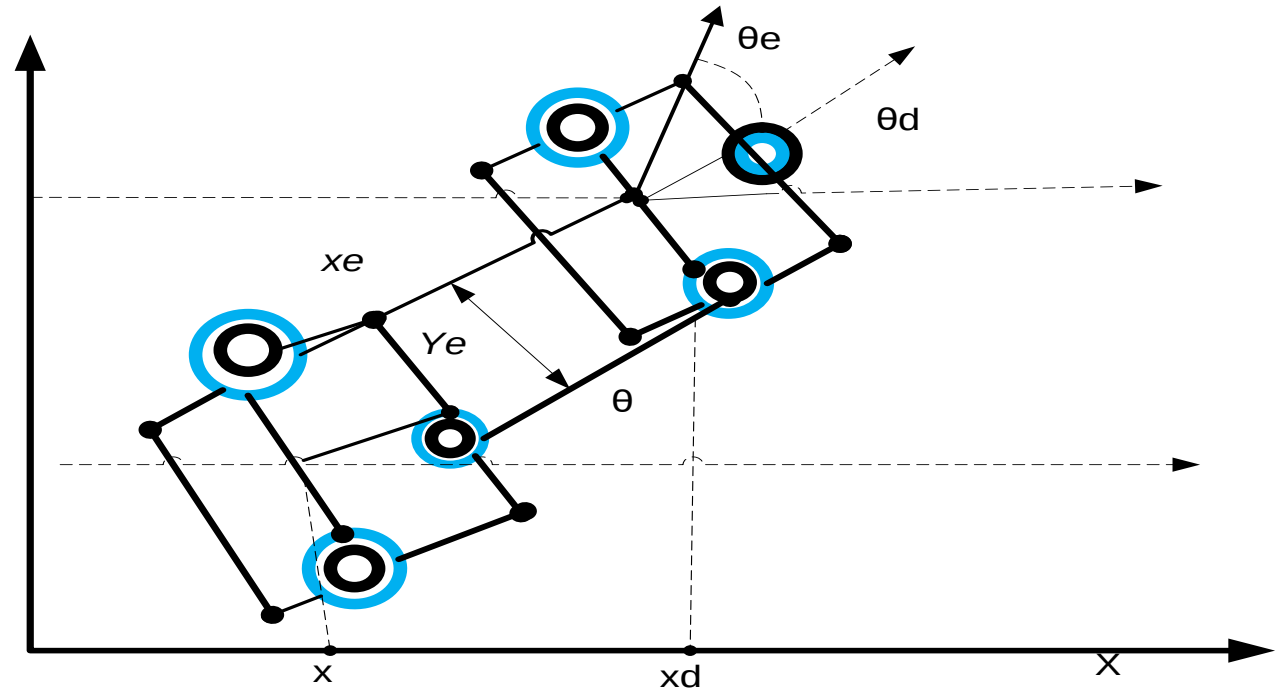

Figure 4. 2: posture error description

Consider a desired trajectory with v_d and ω_d, velocities, as well as path configuration $p_d = (x_d, y_d, \theta_d)^T$. The configuration error in the local coordinate system with respect to the mobile robot system $p_e = (x_e, y_e, \theta_e)^T$ can be expressed as using [40].

$$p = \begin{pmatrix} x_e \\ y_e \\ \theta_e \end{pmatrix} = \begin{pmatrix} \cos\theta & \sin\theta & 0 \\ -\sin\theta & \cos\theta & 0 \\ 0 & 0 & 1 \end{pmatrix} \begin{pmatrix} x_d - x \\ y_d - y \\ \theta_d - \theta \end{pmatrix} \tag{4.2}$$

It can be derived by differentiating Eq. (4.2) and substituting Eq. (4.1) into the result as

$$\begin{cases} x_e' = (v_d cos\theta_d - vcos\theta)cos\theta - \omega(x_d - x)\sin\theta + (v_d \sin\theta \ - vsin\theta)sin\theta + \ \omega(y_d - y)\cos\theta \\ y_e' = -(v_d cos\theta_d - vcos\theta)sin\theta - \omega(x_d - x)\cos\theta + (v_d \sin\theta \ - vcos\theta)sin\theta - \omega(y_d - y)\cos\theta \\ \theta_e' = \omega_d - \omega \end{cases} \tag{4.3}$$

Considering Eq. (4.2), the time derivative of the robot's configuration mistake is:

$$p = \begin{pmatrix} x_e' \\ y_e' \\ \theta_e' \end{pmatrix} = \begin{pmatrix} y_e\omega - v + v_d cos\theta_e \\ -x_e\omega + v_d sin\theta_e \\ \omega_d - \omega \end{pmatrix} \tag{4.4}$$

The control is created with the goal of reducing tracking errors to zero by using a global fast terminal sliding mode controller based on the hasty getting law (GTSMCQR) with nonlinear functions in the shape of the sliding surface [44].

The sliding surface of the rotation position error chosen as follows,

$$s_1 = \dot{\theta}_e + \frac{2\alpha}{1+e^{-\eta 1(|\theta_e|-\varepsilon)}}\theta_e + \frac{2\beta}{1+e^{\eta 2(|\theta_e|-\varepsilon)}}|\theta_e|^{\delta} sign(\theta_e) \quad (4.5)$$

Rearranging of equation (4.5),

$$\dot{\theta}_e = -\frac{2\alpha}{1+e^{-\eta 1(|\theta_e|-\varepsilon)}}\theta_e - \frac{2\beta}{1+e^{\eta 2(|\theta_e|-\varepsilon)}}|\theta_e|^{\delta} sign(\theta_e) \quad (4.6)$$

In this scenario, the control rule can be obtained by considering sliding surface equal to zero in order to satisfy conditions [44]:

$$\theta_e' = \omega_d - \omega = -\frac{2\alpha}{1+e^{-\eta 1(|\theta_e|-\varepsilon)}}\theta_e - \frac{2\beta}{1+e^{\eta 2(|\theta_e|-\varepsilon)}}|\theta_e|^{\delta} sign(\theta_e) \quad (4.7)$$

$$\omega = \omega_d + \frac{2\alpha}{1+e^{-\eta 1(|\theta_e|-\varepsilon)}}\theta_e + \frac{2\beta}{1+e^{\eta 2(|\theta_e|-\varepsilon)}}|\theta_e|^{\delta} sign(\theta_e) \quad (4.8)$$

When two more states are added, the error model (4.4) looks like this:

$$x_e' = y_e\omega_d - v + v_d \quad (4.9)$$

$$y_e' = -x_e\omega_d \quad (4.10)$$

By putting,

$$z = x_e - y_e \quad (4.11)$$

The control law may now be determined from the global fast terminal sliding mode by calculating linear velocity [44]:

$$s_2 = \dot{\theta}_e + \frac{2\alpha}{1+e^{-\eta 1(|z|-\varepsilon)}}\theta_e + \frac{2\beta}{1+e^{\eta 2(|z|-\varepsilon)}}|\theta_e|^{\delta} sign(\theta_e) = 0 \quad (4.12)$$

So, the result can be obtained as:

$$\dot{z} = -\frac{2\alpha}{1+e^{-\eta 1(|z|-\varepsilon)}}z - \frac{2\beta}{1+e^{\eta 2(|z|-\varepsilon)}}|z|^{\delta} sign(z) \quad (4.13)$$

By using the equation (4.9) and (4.10):

$$z' = x_e' - y_e' = y\omega_d - v + v_d + x\omega_d \quad (4.14)$$

By introducing (4.13) and (4.14), the control law can be obtained as:

$$z' = x_e' - y_e' = y_e\omega_d - v + v_d + x_e\omega_d =$$

$$-\frac{2\alpha}{1+e^{-\eta 1(|z|-\varepsilon)}}z - \frac{2\beta}{1+e^{\eta 2(|z|-\varepsilon)}}|z|^{\delta} sign(z) \quad (4.15)$$

$$v = y_e\omega_d + v_d + x_e\omega_d + \frac{2\alpha}{1+e^{-\eta 1(|z|-g)}}z + \frac{2\beta}{1+e^{\eta 2(|z|-g}}|z|^{\delta} sign(z) \quad (4.16)$$

The selected switching surface in given as:

$$s = \begin{pmatrix} s_1 \\ s_2 \end{pmatrix} = \begin{pmatrix} \dot{z} + \frac{2\alpha}{1+e^{-\eta 1(|z|-\varepsilon)}}z + \frac{2\beta}{1+e^{\eta 2(|z|-\varepsilon)}}|z|^{\delta} sign(z) \\ \dot{\theta}_e + \frac{2\alpha}{1+e^{-\eta 1(|\theta_e|-\varepsilon)}}\theta_e + \frac{2\beta}{1+e^{\eta 2(|\theta_e|-\varepsilon)}}|\theta_e|^{\delta} sign(\theta_e) \end{pmatrix} \quad (4.17)$$

The control law can be obtained as:

$$q = \begin{pmatrix} v \\ \omega \end{pmatrix} = \begin{pmatrix} y_e\omega_d + v_d + x_e\omega_d + \frac{2\alpha}{1+e^{-\eta 1(|z|-\varepsilon)}} z + \frac{2\beta}{1+e^{\eta 2(|z|-\varepsilon)}} |z|^{\delta} sign(z) \\ \omega_d + \frac{2\alpha}{1+e^{-\eta 1(|\theta_e|-\varepsilon)}} \theta_e + \frac{2\beta}{1+e^{\eta 2(|\theta_e|-\varepsilon)}} |\theta_e|^{\delta} sign(\theta_e) \end{pmatrix} \quad (4.18)$$

Analysis of stability of the control system is shown by selecting the lyapunov function as follows

$$v_1 = 0.5{\theta_e}^2 \quad (4.19)$$

By Differentiating the equation (4.19) is given as:

$$v_1{}' = \theta_e\theta_e{}' = -\frac{2\alpha}{1+e^{-\eta 1(|\theta_e|-\varepsilon)}} {\theta_e}^2 - \frac{2\beta}{1+e^{\eta 2(|\theta_e|-\varepsilon)}} |\theta_e|^{\delta+1} < 0 \quad (4.20)$$

It can be seen that, $v_1 > 0$ and$v_1{}' < 0$. Thus, the error state variables θ_e and $\dot{\theta_e}$ are stabilized at the equilibrium point.

In order test stability of the control system is proved using selecting the lyapunov function as follows

$$v_2 = 0.5z^2 \quad (4.21)$$

By Differentiating the equation (4.19) is given as:

$$v_2{}' = zz' = -\frac{2\alpha}{1+e^{-\eta 1(|z|-\varepsilon)}} z^2 - \frac{2\beta}{1+e^{\eta 2(|z|-\varepsilon)}} |z|^{\delta+1} < 0 \quad (4.22)$$

It can be seen that, $v_2 > 0$ and$v_2{}' < 0$. Thus, the error state variables z and z' are stabilized at the equilibrium point [44].

4.1.2. Dynamic level control design

A universal debauched terminal sliding mode controller based on the hurried fearing law is given by:

$$s = \dot{x} + \frac{2\alpha}{1+e^{-\eta 1(|x|-\varepsilon)}} x + \frac{2\beta}{1+e^{\eta 2(|x|-\varepsilon)}} |x|^{\delta} sign(x) \quad (4.23)$$

Where, $\beta > 0\ and\ p > q$ are positive odd numbers

The A global fast terminal sliding mode controller based on the quick reaching law as:

$$\dot{s} = -k_1|s|^{g_1} sign(s) - k_2|s|^{g_2} sign(s) - (\rho_{max} + \sigma) sign(s) \quad (4.24)$$

Where $g_1 = f_o + f_1 \tanh(s^r) - f_2 \tanh(\lambda s^2)$ and $g_2 = \begin{cases} g, if\ |s| \le 1 \\ 1, if\ |s| > 1 \end{cases}$ such that, $k_1, k_2, \lambda > 0, 0 < f_2 < f_0 < 1, f_1 > 1, g = f_0 + f_1 - f_2 > 1, and\ r$ is positive even number and $\rho_{max} + \sigma$ used to dominate the matching uncertainty disturbance and external disturbances.

Now begin by defining the error which is the difference between reference value and the actual output of the state defined as follows.

$$e_i' = e_{i+1}\ where\ e_i = \theta_{di} - \theta_i \tag{4.25}$$

Equation (4.23) used to choose the sliding surface function of the GTSMCQR so we can choose the sliding surface based on the above tracking errors as follows.

$$s_1 = \dot{e_1} + \frac{2\alpha}{1+e^{-\eta 1(|e_1|-\varepsilon)}} e_1 + \frac{2\beta}{1+e^{\eta 2(|e_1|-\varepsilon)}} |e_1|^{\delta} sign(e_1) \tag{4.26}$$

Where, s_1 sliding surface & e_1 error is for rotational position of right wheel of mobile robot dynamic respectively.

$$s_2 = \dot{e_2} + \frac{2\alpha}{1+e^{-\eta 1(|e_2|-\varepsilon)}} e_2 + \frac{2\beta}{1+e^{\eta 2(|e_2|-\varepsilon)}} |e_2|^{\delta} sign(e_2) \tag{4.27}$$

Where, s_2 sliding surface & e_2 error is for rotational position of left wheel of mobile robot dynamic respectively. The typical choice to achieve the trajectory tracking is designed using as follows:

$$s_i' = -k_{1i}|s_i|^{g_{1i}} sign(s_i) - k_{2i}|s_i|^{g_{2i}} sign(s_i) - (\rho_{max} + \sigma) sign(s_i) \tag{4.28}$$

such that, k_{1i} & $k_{2i} > 0$,

Therefore, substituting dynamics of rotational position of right wheel of mobile robot from equation (3.50) in to equation (4.26) and rearranging the above equation (4.26), the control input torque for right wheel motor will be,

$$\theta_1'' = k_{11}|s_1|^{g_{11}} sign(s_1) + k_{21}|s_1|^{g_{21}} sign(s_1) + \theta_{1d}'' + \frac{2\alpha}{1+e^{-\eta 1(|e_1|-\varepsilon)}} e_1 + \frac{2\beta}{1+e^{\eta 2(|e_1|-\varepsilon)}} |e_1|^{\delta} sign(e_1) + (\rho_{max} + \sigma) sign(s_1) \tag{4.29}$$

Where, $e_1 = \theta_{1d} - \theta_1$.

Similarly, the control signal torque input for left wheel motor can be expressed as follows by substituting dynamics of rotational position of left wheel of mobile robot in equation (3.50).

$$\theta_2'' = k_{12}|s_2|^{g_{12}} sign(s_2) + k_{22}|s_1|^{g_{22}} sign(s_2) + \frac{2\alpha}{1+e^{-\eta 1(|e_2|-\varepsilon)}} e_2 + \frac{2\beta}{1+e^{\eta 2(|e_2|-\varepsilon)}} |e_2|^{\delta} sign(e_2) + \theta_{2d}'' + (\rho_{max} + \sigma) sign(s_2) \tag{4.30}$$

Where, $e_2 = \theta_{d2} - \theta_2$

Stability of designed controller is verified using lyapunov functions as follows

$$v_3 = 0.5{s_1}^2 \tag{4.31}$$

By Differentiating the equation (4.29) is given as:

$$s_1 {s_1}' = -(k_{11}|s_1|^{g_{11}} sign(s_1) + k_{21}|s_1|^{g_{21}} sign(s_1) + \rho_{max} + \sigma - |\rho|)|s_1| < 0 \tag{4.32}$$

Where, $|\rho_{max}| \geq |\rho|$. Thus, $v_3 > 0$ and ${v_3}' < 0$.

Similarly, the stability of second controller tested such that,

$$v_4 = 0.5{s_2}^2 \tag{4.33}$$

$$s_1{s_1}' = -(k_{12}|s_2|^{g_{12}} sign(s_2) + k_{22}|s_2|^{g_{22}} sign(s_2) + \rho_{max} + \sigma - |\rho|)|s_2| < 0 \tag{4.34}$$

Where, $\sigma > 0$. Thus, $v_4 > 0$ and ${v_4}' < 0$.

CHAPTER FIVE
SIMULATION AND RESULT ANALYSIS

5.1. Open loop analysis and results of simulation first phase

An adequate computer package is needed to mimic robotic systems. We carried out the simulations for this project using MATLAB and MATLAB/Simulink, two potent software tools that have been extensively used in robotics research. In order to evaluate the dynamic simulation and assess the system using Mat lab/Simulink simulation, the proposed Langrage dynamic modeling approach for mobile robot dynamics is carried out in this part.

5.1.1. Simulation block diagram for the entire mobile robot dynamic system

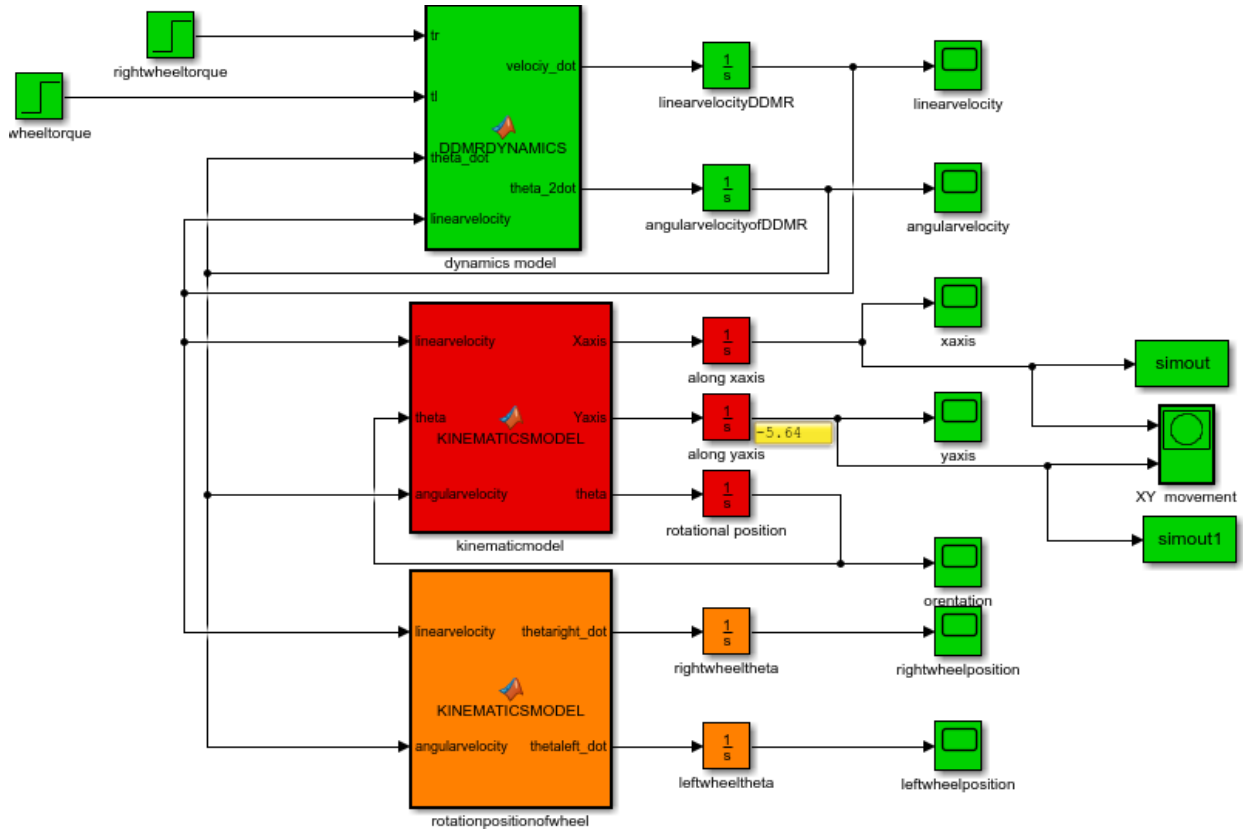

Figure 5.1: The Simulink block diagram to simulate the mechanical element of the robot model

The block diagram above represents the mechanical model of differential drive mobile robot. We simply apply different torques to the mechanical model as the output of the right and left wheel actuators, then assess the robot's motion in reaction to these varying torques. To simulate the robot mechanical model, equations (3.51) to (3.52) for the dynamic model and equation (3.13) for the kinematic model are implemented as MATLAB/SIMULINK, as illustrated in Fig 5.1. After building the model in Mat lab/Simulink, we should define the robot settings and generate different

tests to ensure the model's functionality. Table 5.1 shows the robot parameters used to simulate the model.

Table 5. 1 : Numerical parameter value of DDMR used for simulation [45].

Parameter	Value and unit
m_c	6 kg
m_w	0.5kg
d	0.1m
L	0.5m
r	0.05m
I_c	3kg^2
I_m	0.5kg^2
I_w	0.01875kg^2

Under this section, the impact of input on output state by calculating input for each wheel, primarily the right and left wheels of a mobile robot, using torque inputs.

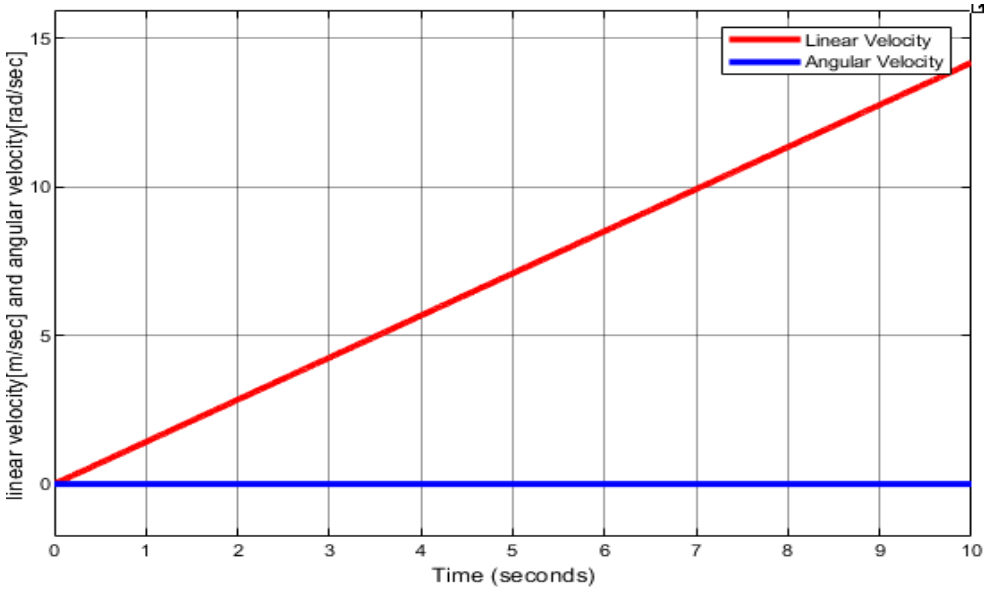

Figure 5.2: Linear and angular velocity

We can observe from Fig. 5.2 that the differential drive mobile robot travels along the XY plane at a linear and angular velocity. As the rotational position of the DDMR will be equal to zero when

both wheels are activated with an equal 0.78Nm of torque, the angular velocity along the XY plane will also be equal to zero, causing the robot to accelerate only in the direction of the X axis.

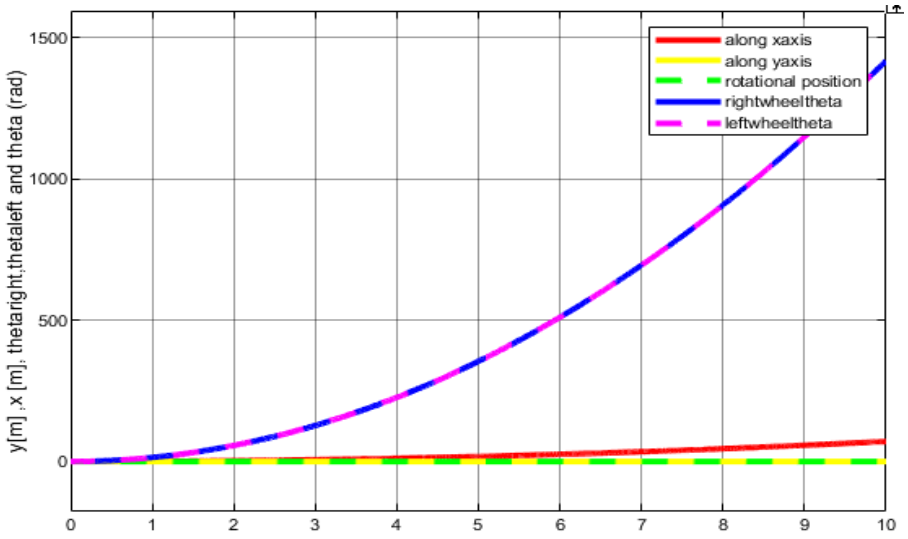

Figure 5.3: X axis, Y axis, rotational position, rotational position (left wheel theta) and rotational position (right wheel theta) under 0.78Nm torque input

According to Fig. 5.3, the mobile robot only moves along the X axis and the DDMR's translational position along the Y axis is zero. Due to the mobile robot moving forward along the X axis, its rotational position was zero. Finally, from Fig. 5.4, the application of a constant torque of 0.78Nm caused the mobile robot to move forward as shown along the XY plane. In this scenario, the robot travels around 72 meters in 10 seconds, with a velocity of 7.5 meters per second.

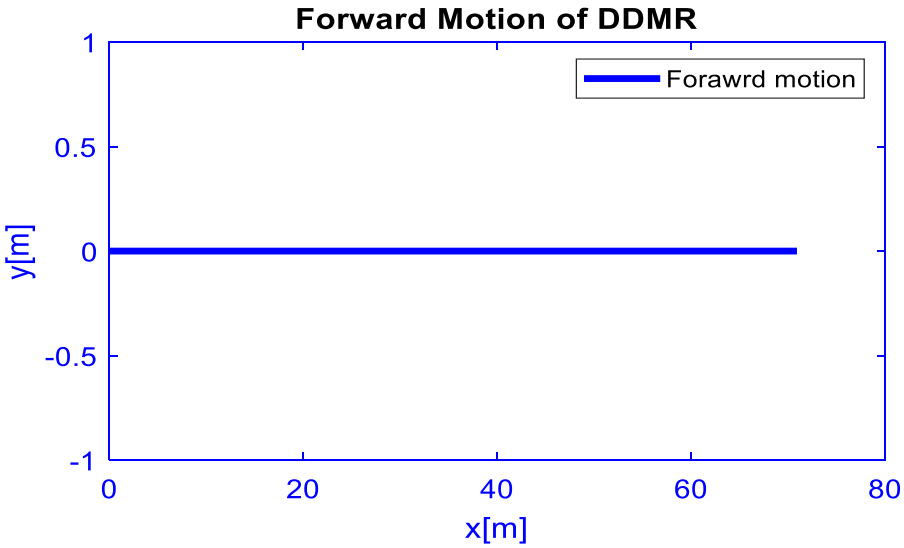

Figure 5.4: Forward motion by applying positive torques of 0.78Nm to each wheel

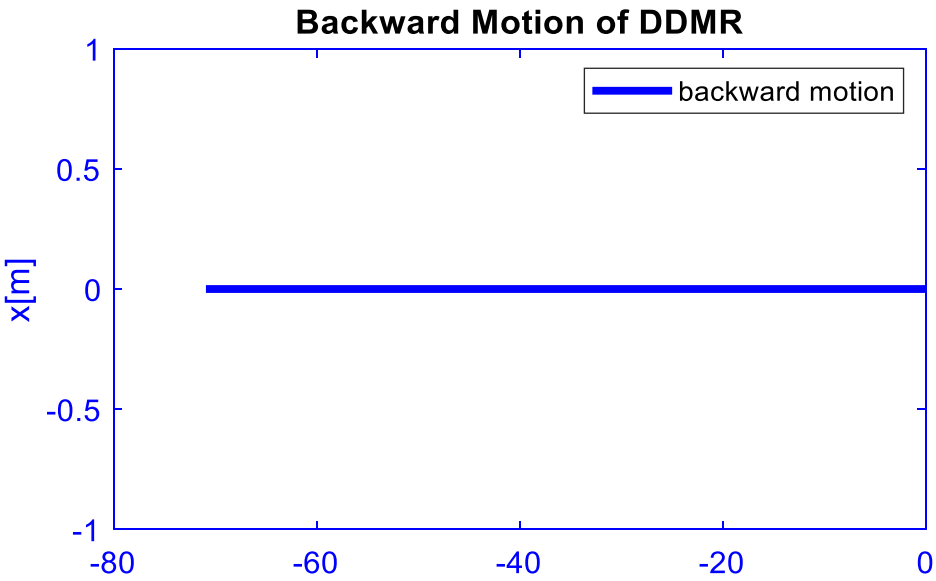

Figure 5.5: backward motion by applying negative torques of -0.78Nm to each wheel

As seen in Fig. 5.5, the robot moves the same amount i.e. 72m, as it does when moving forward, depending on the amount of negative torque given to each of the DDMR wheels and the associated location of each wheel's rotation.

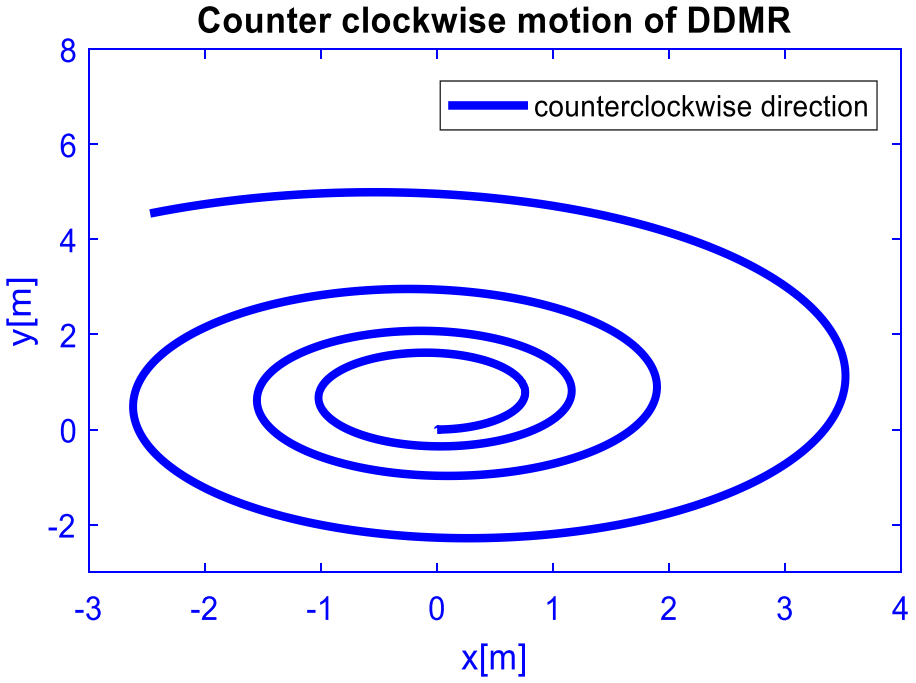

Figure 5.6: Counter Clockwise Motion

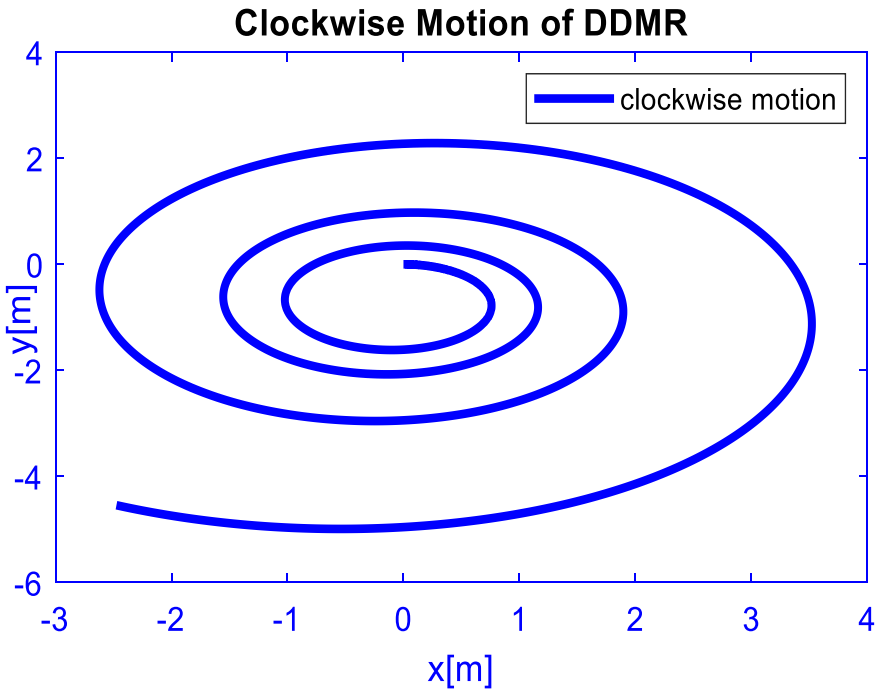

Figure 5.7: Clockwise Motion of DDMR

We explain the motion of a mobile robot in Figs. 5.6 and 5.7 when only one wheel is moved by a motor, and we can see from the graph that the robot moves in opposite directions when just the left and right wheels are moved, respectively.

5.2. Simulation result of the overall tracking control for mobile robot 2nd phase

This part uses Mat lab/Simulink to develop the suggested controller approach for the mobile robot in order to simulate the system's stability and validity. The MATLAB program was chosen to simulate the suggested control and delineate the motion of the mobile robot. In this section, using computer simulation in MATLAB/SIMULINK, we assess the proposed controller's capacity to stabilize the mobile robot while taking into account various time parameterized reference signals for trajectory tracking control system.

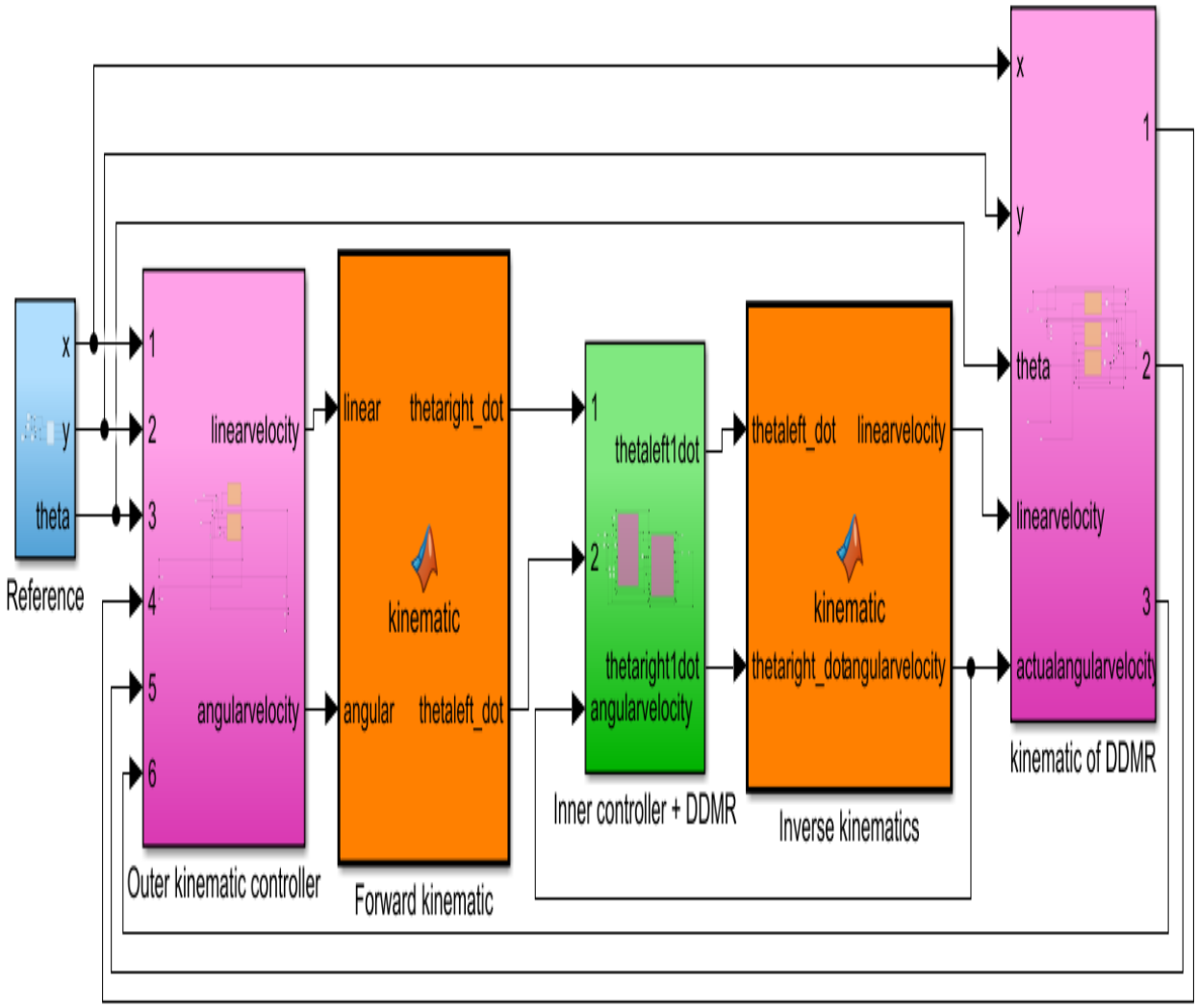

Figure 5.8: Simulink block diagram for overall trajectory tracking control system

As shown in Simulink block in Fig.5.8 above, we have the following main blocks, namely,

- Kinematic level controller (outer loop) for DDMR.
- Forward and inverse kinematics of differential drive mobile robot
- Dynamic controller (inner loop) with dynamic model of DDMR for mobile robot

In this section, we have seen in detail that the proposed control system for tracking performance by giving desired trajectories to states. The following figures show the performance of the NGFSMCNQ and NGFSMC controller performance for each of all states independently at the same time.

In this thesis, the reference trajectories by selected for simulation purpose are:

Table 5. 2 : reference trajectory

Reference trajectory controller parameter	Unit
$v_{r=2}$	m/sec
$\omega_{r=2}$	rad/sec
$xd(t) = 1 + \cos(t)$	m
$yd(t) = 1 + \sin(t)$	m

Both the controller settings for the dynamic controller (inner controller) and the controller parameters for the design of the kinematic level (outer controller) for the mobile robot platform are manually chosen.

Table 5. 3 : Controller parameters [44]

Parameters of proposed controller for DDMR	
Inner controller(NGFSMCNQ)	Outer controller(NGFSMC)
α=5,β=1,$\eta_1 = 1.2, \eta_2 = 1.4,\ \varepsilon = 1$ and $\delta = 0.6$	α=5,β=1,$\eta_1 = 1.2, \eta_2 = 1.4,\ \varepsilon = 1, \sigma = 0.6$ for rotational position of DDMR
$f_o = 0.5, f_1 = 1.3,\ f_2 = 0.5, k_1 = 2, k_2 = 3$ $r = 600, \lambda = 400, \sigma = 0.5$ and $\rho_{max} \geq \lvert\rho\rvert = 10$, where, ρ matching uncertainty disturbance	α=10,β=1,$\eta_1 = 1.2, \eta_2 = 1.4,\ \varepsilon = 1, \sigma = 0.6$ for translational position of DDMR

Demonstration of the control system is evaluated for various initial conditions, where the starting position of the mobile is as follows. The simulation time for trajectory tracking is 10 seconds if the mobile robot starts from its original position with an orientation error of (2m, 1m, pi/6 rad), and the suggested control can implement the tracking system whenever it is desired.

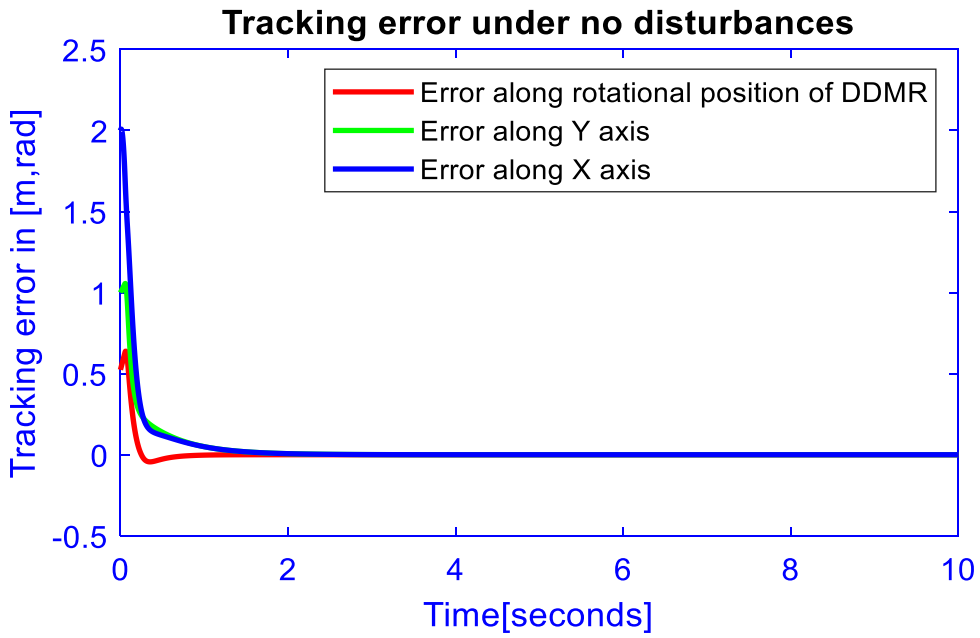

Figure 5.9: Tracking Along X, Y and Theta

The tracking performance of the controller along the x and y axes is shown in Fig. 5.9. Starting from the initial condition given, the tracking error's error along rotational position and translational position will eventually approach zero for both translational position and rotational position. After utilizing NGFTSMC, the tracking error along the three positions approaches zero, allowing DDMR to achieve perfect tracking.

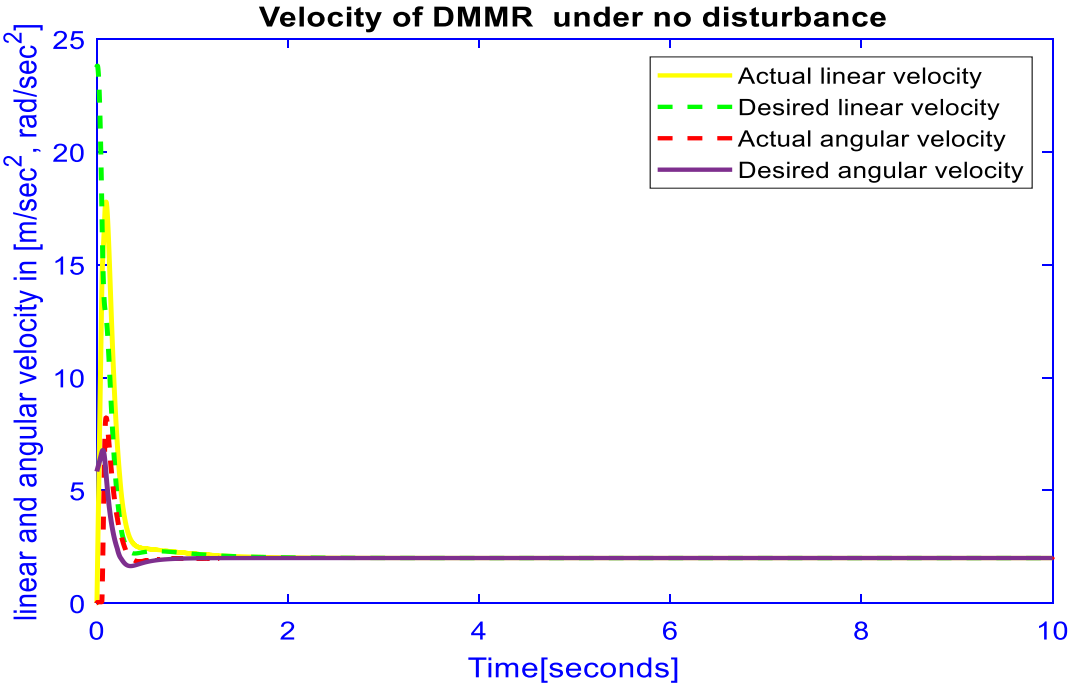

Figure 5.10: Angular and Linear Velocity

Similarly, form Fig.5.10, we can see the control input angular and linear velocity required to achieve the goals starting from zero initial point and we can see that both v and ω are approach to desired velocity 2 rad/sec and 2 m/sec by using inner dynamic NGTSCMNQ controller. Actual linear and angular velocity are output of NGFTSCMNQ controller whereas, desired linear and angular velocity are output of outer kinematic NGFTSMC controller as proposed in this thesis.

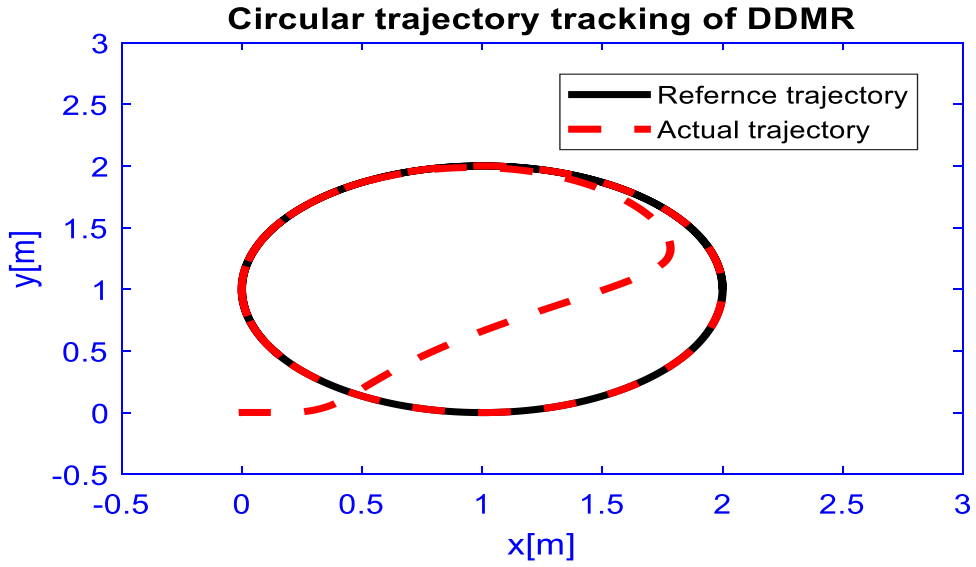

Figure 5.11: Circular trajectory starting from point (0, 0)

Fig 5.11. Indicates the motion mobile robot starting from the given initial position to desired trajectory using the proposed controller. As indicated in this simulation result mobile robots will achieve desired trajectory just after moves nearly 2m.

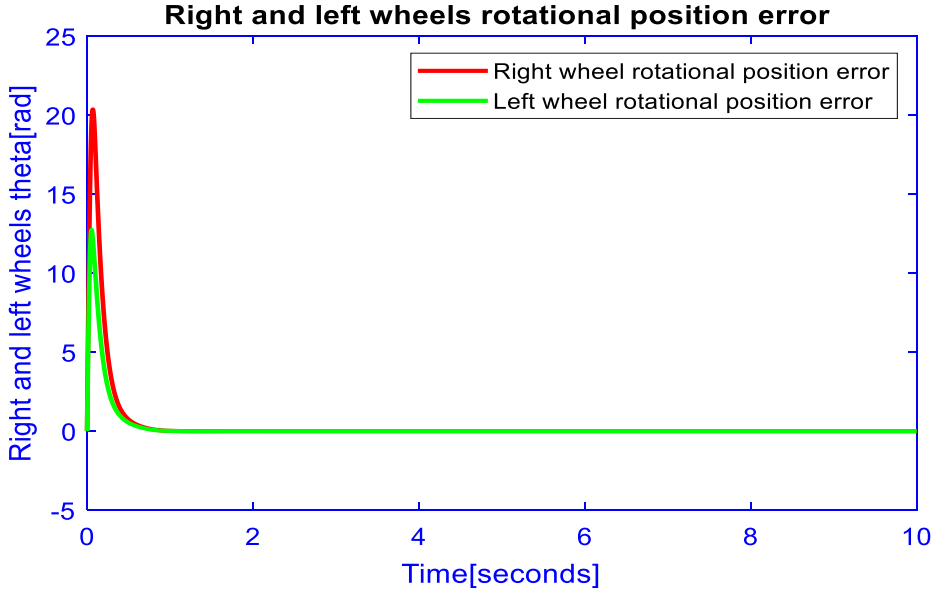

Figure 5.12: Inner controller tracking error of right and left wheel

In order to reduce the inaccuracy between each wheel's rotational locations in a finite manner, the inner controller's performance is shown in Fig. 5.12 using NGFTSMCNQ. As a result, as shown in Fig. 5.11, the kinematic controller generates the desired linear and angular velocity of each wheel to achieve tracking of the reference trajectory. However, since mobile robots cannot be controlled directly in terms of velocity, an inner loop dynamic controller will produce the desired torques for each wheel based on the difference between the actual and desired velocity. In order to reduce the difference between the desired and actual values of rotational position, the inner loop controller is first created at the rotational position level using forward kinematic. Then, using inverse kinematic, the real velocity is retrieved from the inner loop controller. Then, unless DDMR dynamics will affect the motion of the platform if only a kinematic level controller is intended to control the motion of the DDMR, the difference between the desired angular velocity and the actual angular velocity from the vehicle dynamic is applied to the dynamic controller so that the difference between them becomes zero.

Figure 5.13: Torque control input for right and Left motor.

In order to track both angular and linear velocity using an inner loop dynamic controller, it is initially necessary to apply approximately 150Nm and 150Nm of torque control input to the right motor and left motor, respectively. This will ensure that the actual velocity is equal to the desired velocity.

The simulation time for trajectory tracking is 10 seconds assuming that the mobile robot starts from its original position and has an orientation error of 1,0 pi/3rad. The suggested control can implement the tracking system whenever it is desired.

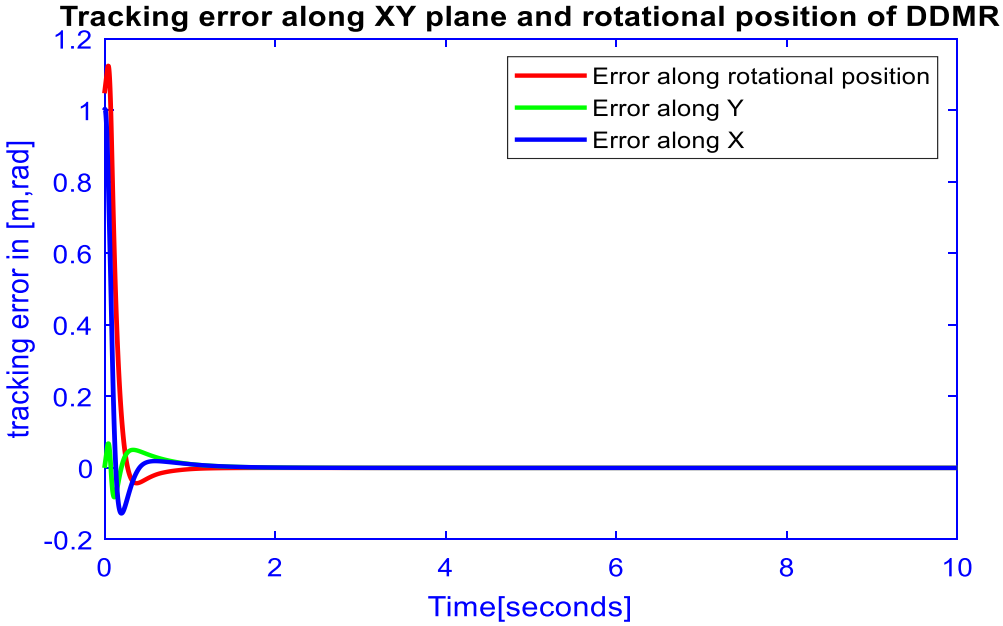

Figure 5.14: Tracking error along XY plane

In case of Fig 5.14, similarly, the mobile robot starts from give initial position and approach to the desired trajectory with a finite time and high precision. Therefore, the proposed controller is able achieve the tracking of the desired trajectory very well and fast response time.

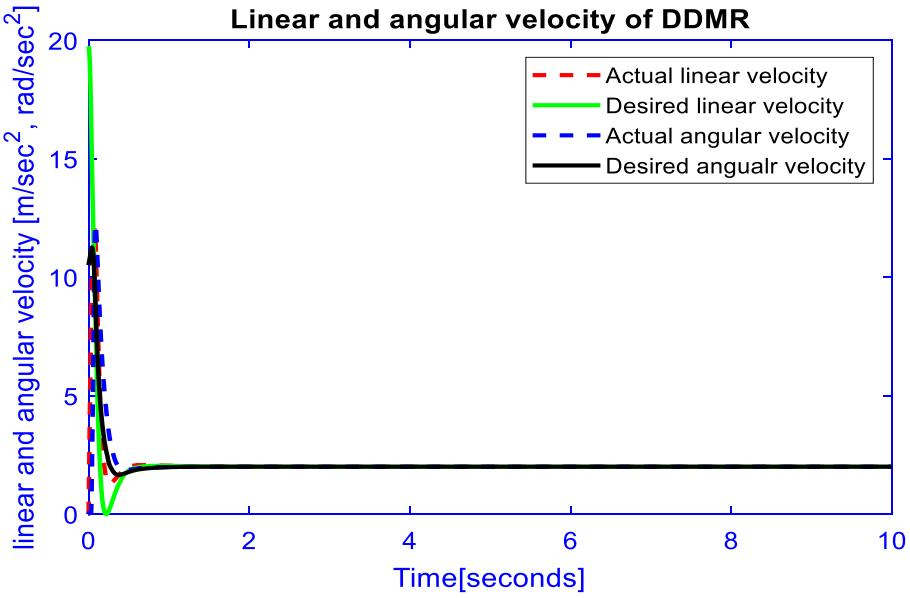

Figure 5.15: linear and angular velocity

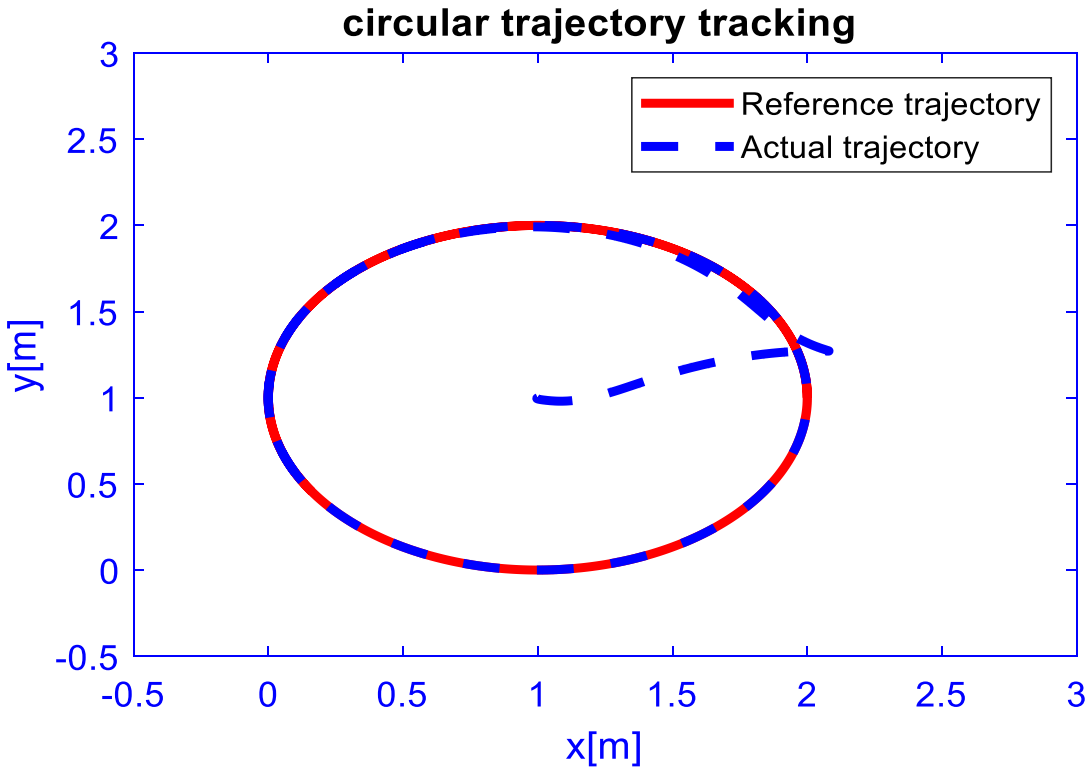

Figure 5.16: Circular tracking starting from point (1m, 1m)

Similarly, from fig. 5.15 and 16, the mobile robot starts from another points and approach given points in finite time with fast and high precise control system.

5.3. Control system under matching model uncertainty and random external disturbance

Random Gaussian disturbances and matching mode uncertainty were applied to each wheel in order to verify the control system's robustness. The left and right wheels of the mobile robot are subjected to the matching model uncertainty (internal disturbance) and external random disturbance as follows.

Table 5. 4 : Random external and internal (model uncertainty) disturbance values [44]

Dynamics	Matching model uncertainty disturbance	External Gaussian disturbance
Right wheel rotational position	$\rho = \sin(20t)$	Variance =10, seed =0 and mean=0
Left wheel rotational position	$\rho = \sin(20t)$	Variance = 10, seed =0 and mean=0

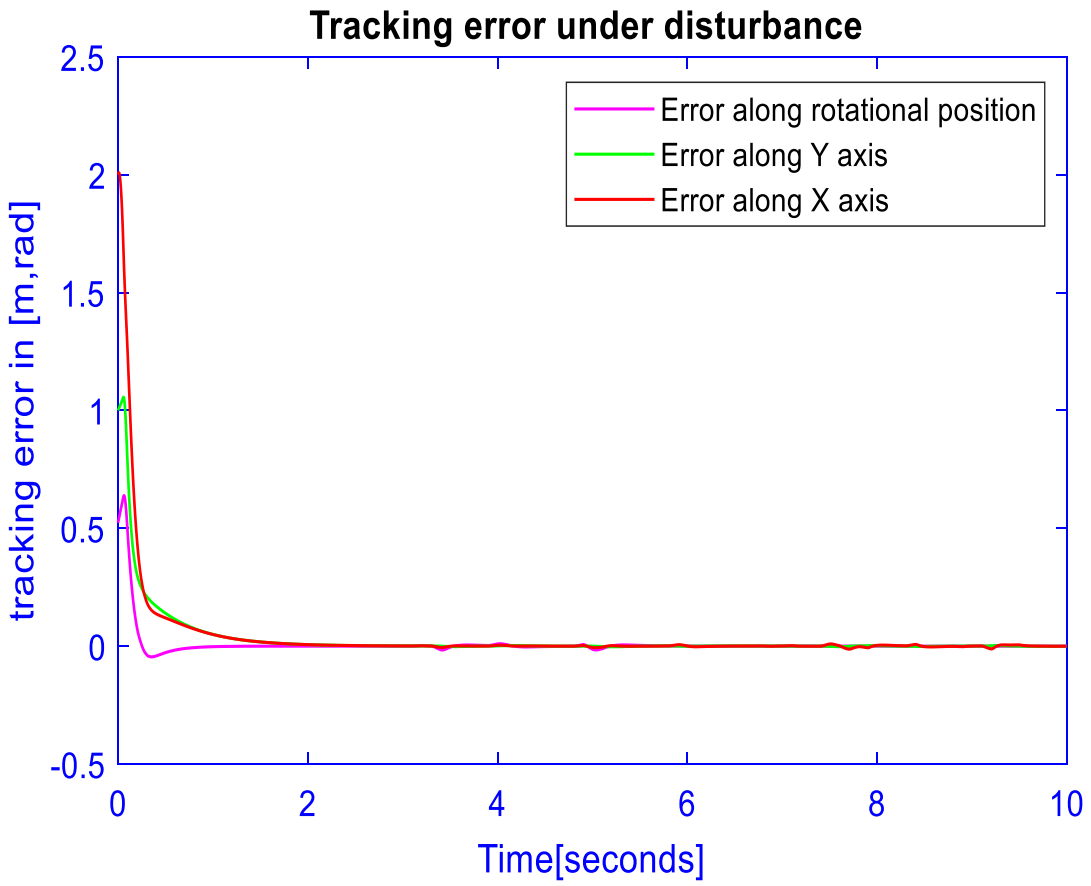

Figure 5.17: Tracking error under both model uncertainty and external disturbances

According to the simulation results shown in Fig. 5.17, the slide mode controller's main advantage is its robustness to both internal and external disturbances. This is demonstrated in tracking error, uncertainty disturbance of sin(20t) is applied to mobile robot dynamics, and random Gaussian disturbance is applied to both torque control output at t=3sec for the right wheel actuator torque and t=5sec for the left wheel actuator torque. However, the suggested controller is completely unaffected by model uncertainty. Tracking error abruptly increases throughout the xy plane and the rotational position of the DDMR in the event that an external Gaussian disturbance is delivered to the right wheel after 3 seconds as illustrated above in Fig. 5.17. However, the NGFTSMCNQ controller responds appropriately and, as seen, reduces error along three coordinates to zeros in a finite amount of time. Similarly, when external disturbance applied at left wheel after 5seconds the tracking errors accidentally increase and becomes zeros according to specified parameters of controllers.

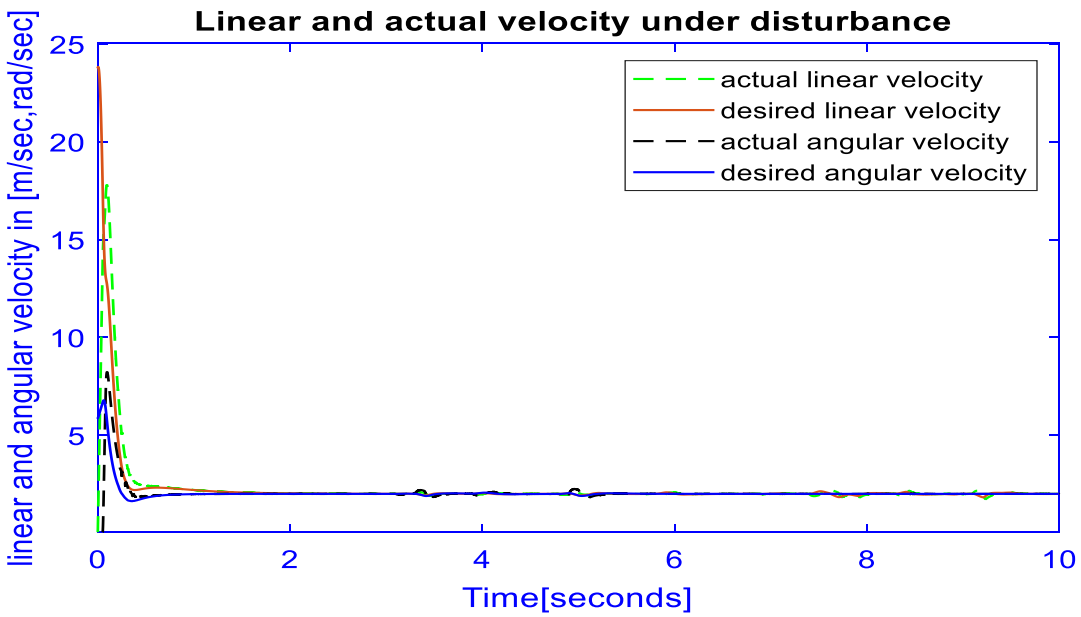

Figure 5.18: linear and angular velocity dynamic controller under external disturbance.

The error between the actual and desired velocities is somewhat influenced by random external disturbance, as shown in Fig. 5.18, but a novel global fast terminal sliding mode control with a novel quick reaching technique causes the error to abruptly return to zero, as demonstrated in the simulation above. However, the controller is completely robust with regard to model uncertainty, or internal disturbance. Therefore, as can be seen from the simulation result above, the objective is met.

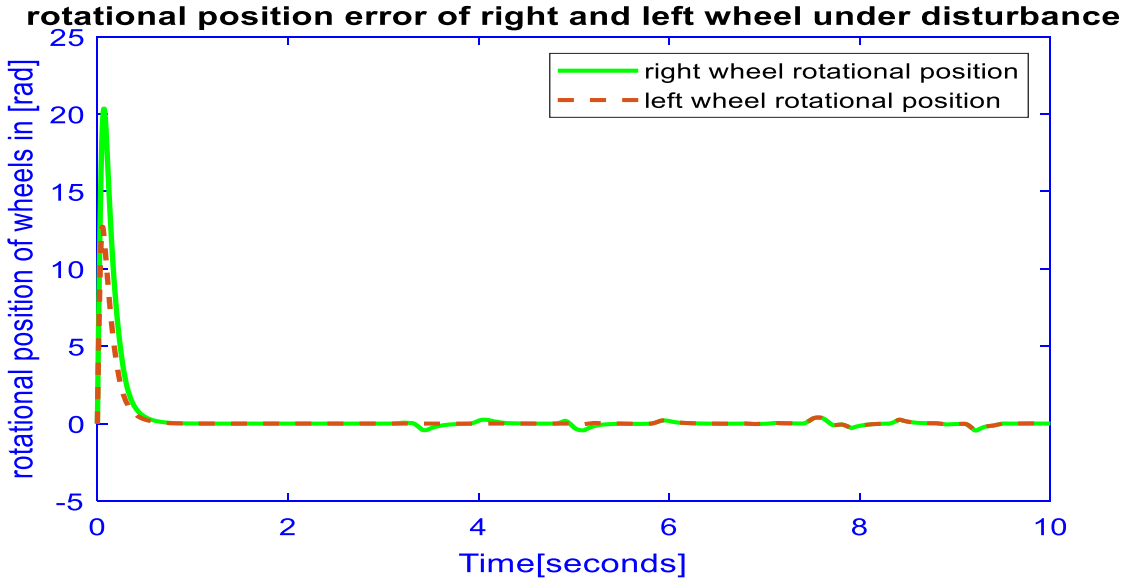

.

Figure 5.19: Rotational position of each wheels under disturbances

From fig 5.19, inner NGFTSMCNQ will rejects both disturbances after random disturbance is applied at 3secs for right wheel and 5secs for left wheel. As also indicated in fig. 5.18 and 19, the inner controller insensitivity to internal disturbance due to model uncertainty

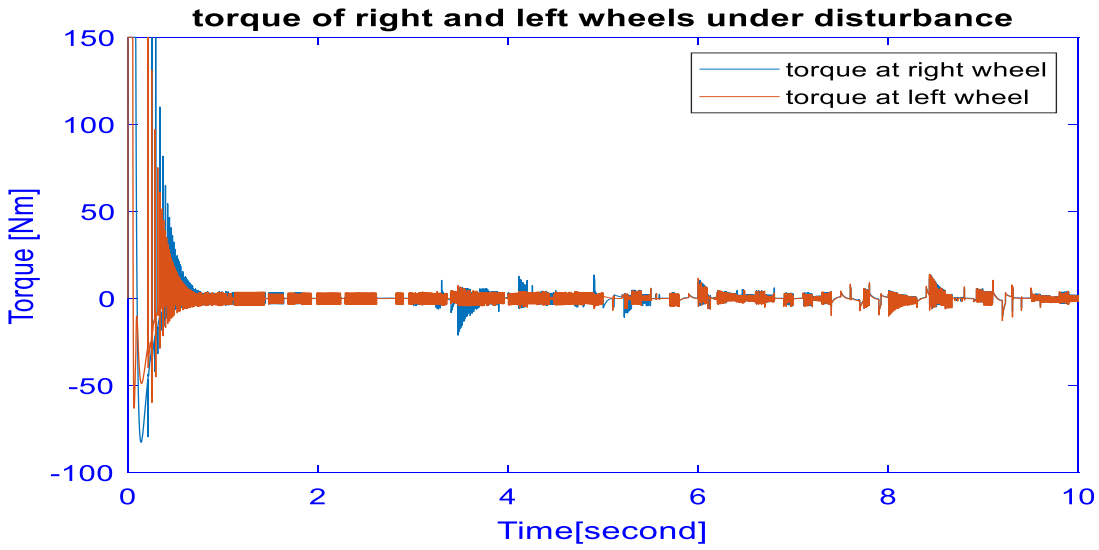

Figure 5.20: Torque both wheels under uncertainty and external disturbances

The starting magnitude of 150Nm is the amount of torque needed to produce the trajectory tracking depicted in Fig. 5.20 for both the right and left wheels. As shown in Fig. 5.21, a mobile robot utilizing the suggested controller is capable of achieving the desired trajectory in the presence of both internal and external disturbances. To bring the error back to zeros, the torque control will behave as indicated in high frequency due to random Gaussian external disturbance variation. In reality, the magnitude of the torque at each wheel fluctuates in response to outside disturbances.

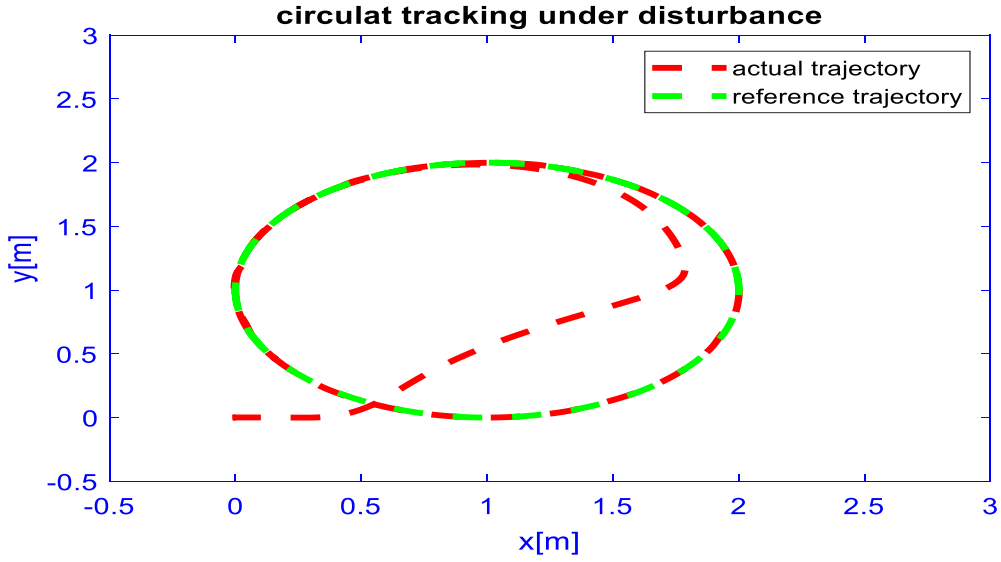

Figure 5.21: Circular trajectory tracking under disturbances

Last but not least, as can be seen in Fig. 5.22, the sliding surface of the global fast terminal sliding mode control system is free from oscillation due to switching function, allowing us to physically implement using different materials for hardware implementation, such as electronics and actuators, without causing damage to those materials. Finally, the suggested controller for differential drive mobile robots with respect to chattering phenomena satisfies another goal of the thesis.

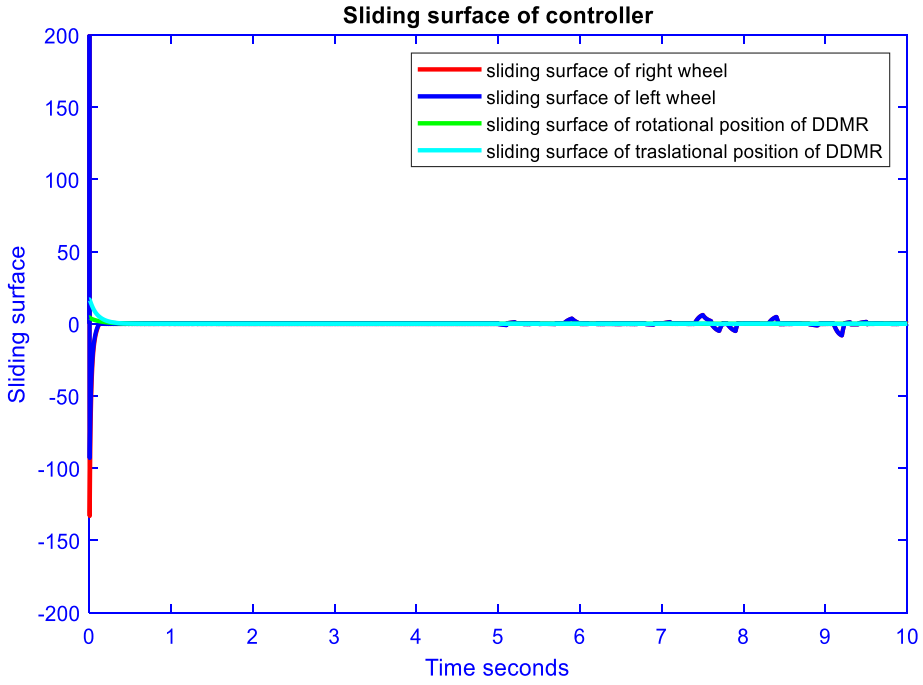

Figure 5.22: Sliding surface inner and outer controller

CHAPTER SIX

CONCLUSION AND FUTURE WORK

6.1. Conclusion

This thesis proposes a control rule for tracking the trajectory of a Nonholonomic mobile robot and derives the dynamics of a differential drive mobile robot using the Langrage formulation. First, a language-based energy-based technique is used to determine the dynamics of DDMR. Then, for the kinematic controller, the tracking control for the DDMR is created to accomplish the required reference trajectory such that the angle error and posture error come to zeros utilizing a finite time global fast terminal sliding mode Similar to this, the dynamic level control system of a mobile robot is created based on the desired velocity from the kinematic controller, corresponding rotation position of each wheel obtained using the kinematic of the mobile robot, then, inner loop controller will ensure trajectory tracking so that error between the actual and desired rotation position is zero in a set amount of time, using global fast terminal sliding mode with quick reaching controller with significant chattering reductions. As a result, the convergence rate, accuracy, and chattering phenomena are improved by three control rules of the linear, angular, and rotational position of wheels. Additionally, the controller's architecture is resilient to both model uncertainty and outside disruption. Finally, the simulation results demonstrate that the suggested control works as expected and may quickly achieve good tracking error convergence.

6.2. Future Work

The following suggestions are recommended for future works

- Modelling of mobile robot with slip
- For further design and evaluation on application area such as welding task, painting robot, plantation robot, inspection robot and etc.
- Navigation and collision avoidance or localization of mobile robot can also be perused.

Additionally, a very interesting development of this study would be to build the planned controller in hardware utilizing a digital control system on a microcontroller.

Reference

[1] K. DO, "bounded controller for global path tracking of unicycle type mobile robot," robot and autonomous system, vol. 61, pp. 775-784, 2013.

[2] X. Gao, L. Yan, and C. Gerada, "modeling and analysis in trajectory tracking control for wheeled mobile robots with wheel skidding and slipping: disturbance rejection perspective," Actuators, 10, 222, 2021.

[3] R. D. a. A. B. .. O. Mohareri, "indirect adpative tracking control of mobile robot via nueral networks," neurocomputing, vol. 88, pp. 54-66, 2012.

[4] D. W. B. a. M. M. D. N. A. Martins, "neural dynamics control of a Nonholonomic mobile robot incorporating the actuator dynamics," CIMCA, IAWTIC and ISE, pp. 563-568, 2008.

[5] T. d. a. S. Taganamathar, "control of nonholonomic mobile robot formutions backstepping kinematics in to dynamcis," in IEEE, singapore, 2007.

[6] W. Benaziza, N. Slimane and A. Mallem, "Mobile robot trajectory tracking using terminal sliding mode control," 6th International Conference on Systems and Control (ICSC), Banta, pp. 538-542, 2017.

[7] S. D. L. C.-A. A. B. a. S. C. Gh. Zidani, "back stepping Controller for a Wheeled Mobile Robot," in IEEE, Sousse, Tunisia April 28-30, 2015.

[8] M. Q. Zaman and H.-M. Wu, "Fuzzy Target Reaching Control of a Differential Drive Mobile Robot Subject to Friction Torques," in 2020 20th International Conference on Control, Automation and Systems (ICCAS), Busan, Korea (South), 2020.

[9] A. T. M. Vinod Raj N, "Design, Simulation and Implementation of Cascaded Path Tracking Controller for a Differential Drive Mobile Robot," in 2015 International Conference on Advances in Computing, Communications and Informatics (ICACCI), Calicut, India, 2015.

[10] N. C. p. a. M. S.l, "Robust Controller for Trajectory Tracking of a Mobile Robot," in 1st IEEE International Conference on Power Electronics. Intelligent Control and Energy Systems (ICPEICES-2016), Calicut, India, 2016.

[11] K. P. P. F. H. S. S. T. P. d. C. a. L. S. Thiago de A. Ushikoshi, "Fuzzy Maneuvering Controller applied to a Dynamic Model of a Differential Drive Mobile Robot," IEEE, 2018.

[12] P. D. Pour, K. M. Alsayegh and M. A. Jaradat, "Type-2 Fuzzy Adaptive PID Controller for Differential Drive Mobile Robot: A Mechatronics Approach," in 2022 Advances in Science and Engineering Technology International Conferences (ASET), Dubai, United Arab Emirates, 2022.

[13] R. Singh, G. Singh and V. Kumar, "Control of closed-loop differential drive mobile robot using forward and reverse Kinematics," in 2020 Third International Conference on Smart Systems and Inventive Technology (ICSSIT), Tirunelveli, India, 2020.

[14] Fukao T., Nakagawa H., and Adachi N. Adaptive Tracking Control of a Nonholonomic Mobile Robot, IEEE Transactions on Robotics and Automation, 16(5), 609-615, 2000.

[15] Kolmanovsky I. and McClamroch N. H. Development in Nonholonomic Control Problems, IEEE Control Systems, 20-36, 1995

[16] Brockett R.W. Asymptotic Stability and Feedback Stabilization, Differential Geometric Control Theory, Birkhauser, Boston, 181–191, 1983.

[17] Canudas deWit C., Khennouf H., Samson C. and Sordalen O. Nonlinear Control Design for Mobile Robots. Recent Trends in Mobile Robotics, Vol. 11, World Scientific Series in Robotics and Automated Systems, 121-156, 1993

[18] Godhavn J. and Egeland O. A Lyapunov Approach to Exponential Stabilization of Nonholonomic Systems in Power Form, IEEE Transactions on Automatic Control, 42(7), 1028-1032, 1997.

[19] Aguiar A., Atassi A. and Pascoal A. Regulation of a Nonholonomic Dynamic Wheeled Mobile Robot with Parametric Modeling Uncertainty Using Lyapunov Function, Proc. 39th IEEE Conference on Decision and Control, Sidney, Australia, 2995–3000, 2000.

[20] Canudas de Wit C. and Sordalen O. Exponential Stabilization of Mobile Robots with Nonholonomic Constraints, IEEE Transactions on Automatic Control, 37(11), 17911797,1992.

[21] Hespanha J., Morse A. S. Stabilization of Nonholonomic Integrators via Logic Based Switching. Automatica, Special Issue on Hybrid Systems, 35(3), 385-393, 1999.

[22] Freund E. and Mayr R. Nonlinear Path Control in Automated Vehicle Guidance, IEEE Transactions on Robotics and Automation, 13(1), 49-60, 1997.

[23] Walsh G., Tilbury D., Sastry S., Murray R. and Laumond J.P. Stabilization of Trajectories for Systems with Nonholonomic Constraints, IEEE Transactions of Automatic Control, 39(1), 216-222, 1994.

[24] Fierro R. and Lewis F. Control of a Nonholonomic Mobile Robot: Backstepping Kinematics into Dynamics, Proc. 34th IEEE Conference on Decision and Control, New Orleans, LA, USA, 3805-3810,1995.

[25] L. Jiukin, Sliding Mode Control Using Matlab, beinjig, Chaina: Elsevier, 2017.

[26] Jinkun Liu and Xinhua Wang, Advanced Sliding Mode Control for Mechanical Systems, Dordrecht, London, New York: Springer, 2014.

[27] Nabil Derbel, Jawhar Ghommam and Quanmin Zhu, Applications of Sliding Mode Control, Singapore: Springer, 2017.

[28] Utkin, V. I. Variable Structure Systems with Sliding Mode. IEEE Transactions on Automatic Control, 22(2), 212-222, 1997.

[29] Utkin, V. I. and Young, K. D. (1978). Method for Constructing Discontinuity Planes in Multidimensional Variable Structure Systems. Automation and Remote Control, 39(10), 1466-1470, 1978.

[30] Slotine, J. J. and Sastry, S. S. Tracking Control of Non-linear Systems Using Sliding Surfaces, with Application to Robot Manipulators. Massachusetts Institute of Technology, Cambridge MA 02139, Technical Report LIDS-P-1264, 1-54, 1982.

[31] Slotine, J. J. and Li, W. Applied Nonlinear Control. Prentice-Hall, Inc, Inglewood Cliffs, New Jersey, 1991

[32] Utkin, V. I. Sliding Modes in Control Optimization. New York, Springer-Verlag,1992.

[33] C. Mu, W. Xu, C. Sun, on switching manifold design for terminal sliding mode control, J. Frankl. Inst. 353 (7) 1553–1572,2016.

[34] V.T. Haimo, Finite time controllers, SIAM J. Control Optim. 24 (4) 760–770, 1986.

[35] S.P. Bhat, D.S. Bernstein, Finite-time stability of homogeneous systems, in: Proceedings of the American Control Conference, vol. 4, American Automatic Control Council, pp. 2513–2514, 1997.

[36] Park KB, Tsuiji T. Terminal sliding mode control of second-order nonlinear uncertain systems, International Journal of Robust and Nonlinear Control, 9 (11): 769 _ 780, 1999.

[37] Hung, J. Y., Gao, W. and Hung, J. C. Variable Structure Control: A Survey. IEEE Transaction on Industrial Electronics, 40(1), 2-22.1993.

[38] DeClarlo, R.A., Zak, S. H. and Mathews, G. R. Variable Structure Control of Nonlinear Multivariable Systems: A Tutorial. Proceedings of the IEEE, 76(3), 212-232.1988.

[39] Gao, W. and Hung, J. C. Variable Structure Control of Nonlinear Systems: a New Approach. IEEE Transaction on Industrial Electronics, 40(1), 45-55.1993.

[40] Y. Kanayama, Y. Kimura, F. Miyazaki, and T. Noguchi, "A stable tracking control method for an autonomous mobile robot," in Robotics and Automation, 1990.Proceedings., 1990 IEEE International Conference on, pp. 384-389, 1990

[41] R. Thomas, "Sliding Mode Controller for a Quadrotor," University of Victoria, India, 2017.

[42] M. Ahmed, Sliding Mode Control for Switched Mode Power Supplies, Lappeenranta: Lappeenranta University of Technology, December 2004.

[43] D. a. A. A. Hatab, "Dynamic Modelling of Differential-Drive Mobile Robots using Lagrange and Newton-Euler Methodologies: A Unified Framework," Advances in Robotics and automation, vol. 2, no. 2, 2013.

[44] . G. Z. H. O. I. L. M. I. HUIHUI PAN 1, "A Novel Global Fast Terminal Sliding Mode Control Scheme for Second-Order Systems," IEEE ACCESS, vol. 8, 2020.

[45] D. V. P. Ankit Sharma, "Control of Mobile Robot for Trajectory Tracking by Sliding Mode Control Technique," in International Conference on Electrical, Electronics, and Optimization Techniques (ICEEOT) - 2016, Greater noida, India, 2016.

[46] A Backstepping Global Fast Terminal Sliding Mode Control for Trajectory Tracking Control of Industrial Robotic Manipulators

[47] Dynamic Model and Balancing Control for Two-Wheeled Self-Balancing Mobile Robot on the Slopes